National Technical University of Ukraine «Igor Sikorsky Kyiv Polytechnic Institute»

Faculty of electric power engineering and automatics

Department of automation of electromechanical systems and electric drives

«On the rights of the manuscript»
UDC ____

«Defense allowed»

Head of Department
_____ Sergei Peresada
(signature) (Name, Surname)
"___" _____2020

Thesis

of the specialty 141 Electrical Energetics, Electrical Engineering and Electromechanics (Automation of electromechanical systems and electric drives)

on the topic: «Electric vehicle drivetrain based on permanent magnet synchronous motor with loss minimization control algorithm»

Performed: student of II (VI) year, group EP-91mp
(group code)

Pavlo Soroka _____
(name, surname)

Supervisor Associate Professor, Dr.Sc. Ivan Shapoval _____
(post, scientific degree, academic title, name and surname) (signature)

Advisor _____ _____ _____
(chapter) (scientific degree, academic title, name and surname) (signature)

Advisor _____ _____ _____
(chapter) (scientific degree, academic title, name and surname) (signature)

Reviewer Associate Professor, Ph.D. Mykola Reutskyi _____
(post, scientific degree, academic title, name and surname) (signature)

I certify that in this master's thesis there are no borrowings from the works of other authors without corresponding references.
Student _____
(signature)

Kyiv – 2020

DIPLOMA PROJECT INFORMATION

№	Format	Marking	Name	Pages	Note
1	A4		Tasks for the master thesis	2	
2	A4	6.050702.5126.016.EN	Explanatory note	91	
3	A1	6.050702.5126.016.MT	Electric drive block diagram	1	
4	A1	6.050702.5126.016.MT	Power circuit diagram	1	
5	A1	6.050702.5126.016.MT	Control circuit diagram	1	
6	A1	6.050702.5126.016.MT	Results of mathematical modelling - 1	1	
7	A1	6.050702.5126.016.MT	Results of mathematical modelling - 2	1	
8	A1	6.050702.5126.016.MT	Results of mathematical modelling - 3	1	

<table>
<tr><td></td><td></td><td></td><td></td><td colspan="3">6.050702.5126.016.MT</td></tr>
<tr><td></td><td>Name</td><td>Sign</td><td>Date</td><td colspan="3"></td></tr>
<tr><td>Developed</td><td>P. Soroka</td><td></td><td>16.12.20</td><td rowspan="5">Diploma project information</td><td>Page</td><td>Pages</td></tr>
<tr><td>Supervised</td><td>I. Shapoval</td><td></td><td></td><td>2</td><td>93</td></tr>
<tr><td></td><td></td><td></td><td></td><td rowspan="3">NTUU «Igor Sikorsky Kyiv Polytechnic Institute», FEA</td></tr>
<tr><td>N. contr.</td><td></td><td></td><td></td></tr>
<tr><td>Approved</td><td>S. Peresada</td><td></td><td></td></tr>
</table>

Explanatory note

to the graduation project

Topic: Electric vehicle drivetrain based on permanent magnet synchronous motor with loss minimization control algorithm

Kyiv 2020

NATIONAL TECHNICAL UNIVERSITY OF UKRAINE
«IGOR SIKORSKY KYIV POLYTECHNIC INSTITUTE»

Faculty of Electric Power Engineering and Automatics

Department of automation of electromechanical systems and electric drives

Higher education level - the second (master's) in educational and professional program

Specialty 141 Electrical Energetics, Electrical Engineering and Electromechanics (Control, Protection, and Automation of Electric Power Systems)

APPROVED
Head of Department
_____ Sergei Peresada
(signature) (name)

«__» _____December___2020

TASK
for the master's thesis of the student
Pavlo Soroka
(name and surname)

1. Thesis topic: *Electric vehicle drivetrain based on permanent magnet synchronous motor with loss minimization control algorithm*
Supervisor *Ivan Shapoval, Ph.D. Associate Professor*,
(name, surname, scientific degree, academic title)

approved by university order from «__» _____2020 №_____

2. The term of submission of the thesis by the student: *14.12.2020.*

3. Research object: electromechanical processes in electric vehicle drivetrain.

4. Research subject: loss minimization control algorithm of a permanent magnet synchronous motor for electric vehicle applications.

5. The list of tasks to be completed: analysis of existing drivetrain solutions of electric vehicles, an overview of their main elements and parts; electric vehicle traction motor and battery pack calculation; calculation of parameters of electric vehicle drivetrain elements; development of loss minimization control algorithm of permanent magnet synchronous motor for electric vehicle applications; mathematical simulation of the obtained electromechanical system.

6. List of graphic (illustrative) material: sheet 1 – Electric drive block diagram; sheet 2 – Power circuit diagram; sheet 3 – Control circuit diagram; sheet 4,5,6 – Results of mathematical modelling.

7. Indicative list of publications Pavlo Soroka, Ivan Shapoval, "Parameters calculation of traction motor and battery pack for electric vehicle application" // International scientific and technical journal of young scientists, graduate students and students "Modern problems of electric power engineering and automation", - 2020.

8. Master`s chapters advisors

Chapter	Name, surname, advisor`s post	Signature, date	
		the task gave	the task accepted

9. Date of issue of the assignment *02.09.2020.*

Calendar Schedule

№ t/p	The name of the stages of the master's thesis	The term of completion of the stages of the master's thesis	Note
1	Analysis of existing drivetrain solutions of electric vehicles, overview of their main elements and parts.	02.09.2020-21.09.2020	
2	Electric vehicle traction motor and battery pack calculation.	22.09.2020-12.10.2020	
3	Calculation of parameters of electric vehicle drivetrain elements.	13.10.2020-26.10.2020	
4	Development of loss minimization control algorithm of permanent magnet synchronous motor for electric vehicle applications.	11.11.2020-30.11.2020	
5	Mathematical modeling of the obtained electromechanical system.	01.12.2020-07.12.2020	
6	Preparation of explanatory note.	08.12.2020-11.12.2020	

Student _____ Pavlo Soroka
(signature) (name, surname)

Supervisor _____ Ivan Shapoval
(signature) (name, surname)

ABSTRACT

The thesis comprises: 93 pages, 32 figures, 32 tables, and graphical part on 6 pages A1.

The thesis aims to develop the method of calculating the parameters of the electric vehicle drivetrain, based on a permanent magnet synchronous motor.

Parameters of traction motor, battery pack, and control circuit elements of the electric vehicle drivetrain were calculated. Loss minimization control algorithm for interior permanent magnet synchronous motor was developed. Electromechanical system performance characteristics were studied by mathematical simulation. The efficiency of the developed control algorithm was compared with the conventional vector control method.

LOSS MINIMIZATION, PERMANENT MAGNET SYNCHRONOUS MOTOR, MATHEMATICAL MODEL, ELECTRIC DRIVETRAIN, BATTERY

РЕФЕРАТ

Дипломний проект містить: сторінок – 93, рисунків – 32, таблиць – 32 та графічну частину на 6 листах А1.

Метою роботи є розробити алгоритм розрахунку параметрів електроприводу автомобіля на основі синхронного двигуна з постійними магнітами.

В даній дисертації було розраховано параметри тягового двигуна, батареї та елементів кола керування електроприводом електромобіля. Синтезовано алгоритм керування синхронним двигуном з вбудованими постійними магнітами з мінімізацією втрат. Було досліджено динамічні характеристики електромеханічної системи методом математичного моделювання. Було порівняно енергоефективність розробленого методу керування зі звичайним векторним керуванням.

МІНІМІЗАЦІЯ ВТРАТ, СИНХРОННИЙ ДВИГУН З ПОСТІЙНИМИ МАГНІТАМИ, МАТЕМАТИЧНА МОДЕЛЬ, ЕЛЕТКРОПРИВОД, БАТАРЕЯ.

TABLE OF CONTENTS

LIST OF ABBREVIATIONS

EV	Electric vehicle
PMSM	Permanent magnet synchronous motor
IM	Induction motor
SRM	Switched reluctance motor
DC	Direct current
SPMSM	Surface permanent magnet synchronous motor
IPMSM	Interior permanent magnet synchronous motor
FOC	Field Oriented Control
DTC	Direct Torque Control
FWC	Field-weakening Control
MTPA	Maximum torque per ampere
MTPV	Maximum torque per volt
IGBT	Insulated Gate Bipolar Transistor
MCU	Microcontroller unit

INTRODUCTION

Significant energy resources exhaustion, environmental problems, and growing societal concern drew attention to research on electric vehicles all around the world. Cars with internal combustion engines are a significant source of air pollution due to greenhouse gas emissions, have complex construction, and are expensive to maintain. With a much smaller impact on the environment, electric vehicles can be the main type of vehicle in the future. Moreover, recent improvements in technology have significantly increased the energy efficiency and controllability of electric land vehicles.

In electric vehicles, angular velocity and electromagnetic torque are regulated by the control system. In the past few years, the Permanent Magnet Synchronous Motor based drivetrains are of growing interest due to their higher power density and great mass-dimensional characteristics. Although PMSM is more efficient than other types of electric vehicle traction motors, further efficiency improving via implementation of loss-minimization control algorithms will allow to reduce the battery size and increase vehicle power reserve.

Thesis actuality. Since energy efficiency is crucial for electric vehicles, optimal energy-efficient control is one of the most relevant tasks. The greater energy efficiency, the bigger single charge range is and the lower battery capacity needed.

The relation with science programs, themes, and plans. The master thesis is performed in the department of automation of electromechanical systems and electric drives of National Technical University of Ukraine «Igor Sikorsky Kyiv Polytechnic Institute».

Research goals and tasks. The goal is to develop a loss minimization control algorithm of a permanent magnet synchronous motor, which can be used in electric vehicle applications.

Tasks of the thesis:

1. Analysis of existing drivetrain solutions of electric vehicles, overview of their main elements and parts.

2. Electric vehicle traction motor and battery pack calculation
3. Calculation of parameters of electric vehicle drivetrain elements
4. Development of loss minimization control algorithm of permanent magnet synchronous motor for electric vehicle applications.
5. Mathematical simulation of the obtained electromechanical system.

Research object. Electromechanical processes in electric vehicle drivetrain

Research subject. The electromechanical system based on a permanent magnet synchronous motor for electric vehicle applications.

The scientific novelty of obtained results. The algorithm for designing an electric vehicle drivetrain based on a permanent magnet synchronous motor with loss minimization is developed.

Practical application of obtained results. Obtained results can be used for the calculation and selection of drivetrain elements during vehicle modernization or design.

Scientific publications. Part of the results are published in the article:

1. Pavlo Soroka, Ivan Shapoval, “Parameters calculation of traction motor and battery pack for electric vehicle application” // International scientific and technical journal of young scientists, graduate students, and students "Modern problems of electric power engineering and automation", – 2020.

CHAPTER 1. ANALYTICAL OVERVIEW

Today the importance of the transport industry in the world cannot be overemphasized, as it is a vital component of the global economy. However, with the growing environmental concern the fact that the transport sector consumes more than 60% of the oil used each year can't be neglected. Nowadays, one of the most popular and comfortable types of city transport are cars. However, their major disadvantage is that internal combustion engines are the source of greenhouse gas emissions. As reported by [1], around 4.6 tons of carbon dioxide is produced by a typical passenger vehicle every year. Also, conventional vehicles produce other toxic gases, such as nitrous oxide and methane, causing great damage to the environment. Besides, gasoline cars are a quite expensive type of transport, since prices in the oil market are volatile.

Production of energy-efficient traction motors and new electrical materials implementation can be considered as a technological revolution in the field of electric vehicles, as a result of which the number of electric and hybrid vehicles is constantly growing. According to the International Energy Agency, approximately 60 million electric vehicles are expected to be produced by 2030 [2]; according to Bosch experts, 15% of worldwide produced cars will be hybrid by 2025 [3].

Traction motor efficiency is not the only factor that determines the energy efficiency of the whole drivetrain, because the mass, size, and maximum rotation speed of the motor are also crucial parameters. Reduced mass allows to minimize rolling resistance, the smaller size makes it possible to install extra batteries, greater efficiency is the key to increase the single-charge range of the electric vehicle and to facilitate engine cooling.

1.1 Comparison of electric motors for EV application

One of the first steps in an electric vehicle drivetrain system development is traction motor selection. The traction motor is one of the main parts of the electric vehicle drivetrain, as it converts electrical energy into mechanical and vice versa.

When the vehicle is moving, electrical energy from the power supply is converted into mechanical, and during braking electric motor works as a generator, i.e. the kinetic energy of the vehicle is converted into electrical. It is necessary to select an appropriate electric motor because the dynamic performance and power reserve of the electric vehicle greatly depends on the traction motor characteristics, especially its efficiency and weight [4].

Traction motor works in the conditions of frequent accelerations and stops, high speeds, considerable accelerations, and decelerations. Besides, the motor has to be able to work reliably in different environmental conditions, be insensitive to vibrations and overloads. Electric motors for EV applications differ from motors for industrial usage. Traction motors have to [5]:

- produce high torque at low speeds;
- provide high efficiency over a wide torque range;
- be suitable for regenerative braking;
- provide ease of control;
- have high overload capacity, high reliability, and a low weight;
- be suitable for operation over a wide temperature range.

The ideal mechanical characteristic of the traction motor for electric vehicle application provides constant power over the entire speed range. In this case, at any given speed the maximal motor power will be utilized. However, usually in practice, it is necessary to limit the maximum motor torque at low speeds to avoid wheel slipping.

The mechanical characteristic of an internal combustion engine differs: at low speeds torque is low, at medium speeds torque is high and proper fuel combustion is achieved, at high speeds the torque drops. Therefore, in conventional cars with internal combustion engines gearbox is used to provide the required mechanical characteristic.

Modern electric motor control algorithms allow to achieve mechanical characteristic that is close to the ideal, which is shown at Fig. 1.1. Acceleration of the electric car begins at zero traction motor speed. As the rotational speed increases to the rated, the voltage increases to the nominal value, while the flux remains constant and the constant torque is produced. When the motor is operated above the rated speed, the voltage remains constant at the nominal value and the flux must be decreased. The output power is constant, and the torque decreases along the hyperbolic curve in proportion to the speed change.

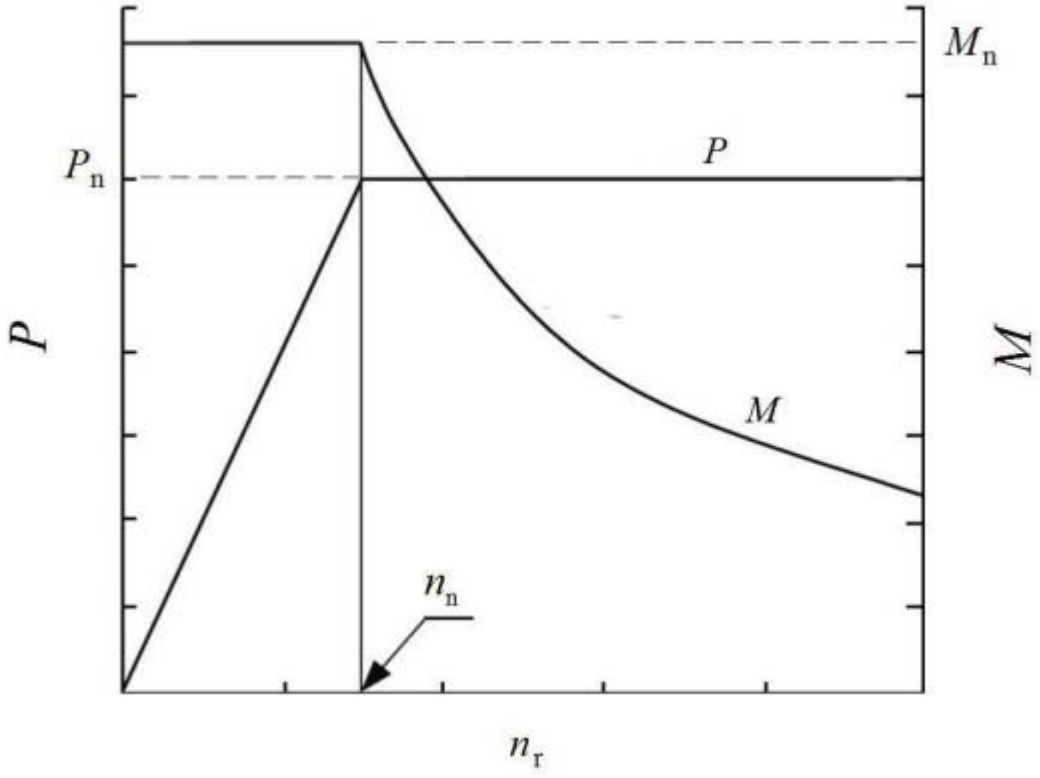

Figure 1.1 – Typical mechanical characteristic of the EV traction motor

The most popular types of electric motors that are used in the EV industry are permanent magnet synchronous motors (PMSM) and induction motors (IM), while switched reluctance motors (SRM) and direct current (DC) motors are receiving less attention.

DC motors were used in the first electric vehicles at the beginning of the 20th century since they offered simple control over a wide speed range, high starting

torque, no reactive power consumption, decoupling of electrical and mechanical processes. However, a significant number of disadvantages, such as the presence of a brush-collector unit, high weight, low efficiency, and complicated maintenance have made DC motors redundant in the automotive industry after the development of the novel vector control strategies of AC motors. However, DC motors can still be used in low-power systems, when a simpler and cheaper electric drivetrain is required.

Induction motors are a fairly common option due to their reliability, lower maintenance costs, and ability to work in more aggressive environments. In vector-controlled IM electrical and mechanical processes are decoupled, and usage of flux weakening control methods in the constant power region makes it possible to extend the operating speed range. Thus, field-oriented control of induction motor with squirrel-cage rotor allows combining the typical advantages of AC machines (simple and cheap construction, absence of brushes) with good starting and control characteristics of a DC motor. Moreover, usually IM drives require no maintenance during all operation period of the electric vehicle. Although IM has a greater mass compared to the PMSM and low energy efficiency, it still can be used as a traction motor, because the motor weight usually does not exceed 2-5% of the total weight of the electric car and is significantly less than the battery weight; also state-of-the-art production technologies allow to decrease losses in newer IM.

Although switched reluctance motors have simple and rigid construction, as well as good torque-speed characteristics, and are easy to control, their disadvantages, namely significant torque ripple and electromagnetic interference, made them not suitable for serial production of electric vehicles [6].

Recently, permanent magnet synchronous motors have become increasingly popular in the automotive industry. A lot of car manufacturers (such as Tesla, Porsche, Nissan, Toyota, Honda, etc.) use PMSM-based drivetrains in their electric vehicles. In this case, as a rule, highly efficient permanent magnets (PM) based on rare earth elements, especially neodymium (Nd), are used. Having highly efficient permanent magnets in construction, these motors have a higher power density,

higher efficiency, and better dynamic performance than induction motors [7]. Besides, they can be operated over a wider speed range, have higher overload capacity and higher torque at low speeds.

1.2 Usage of PMSM in EV drivetrains

As mentioned above, currently of great interest are PMSM-based electric vehicle propulsion systems. This motor is an alternating current machine with a three-phase winding on the stator and permanent magnets mounted on the rotor.

New researches on rare earth elements, used in permanent magnets, led to a significant boost in PMSM development. Nowadays, motors are manufactured in a wide range from relatively small to high power, depending on electric vehicle parameters and desired performance.

There are two types of PMSM, according to the direction of magnetic flux: radial and axial flux PM machines [8]. Radial flux machines with an elongated cylindrical rotor are most commonly used. However, compact disc-shaped construction and higher power density of axial flux machines made them useful in specific cases. But it should be mentioned that production of axial flux machines is more complicated and expensive compared to radial flux machines.

Also, PMSM is divided into internal and external rotor machines, which is illustrated in Fig. 1.2. The most common type for electric vehicle application is internal rotor motors since external rotor motors have higher rotor inertia (which is suitable for mechanisms that require constant rotation speed, such as fans, but not for automobiles).

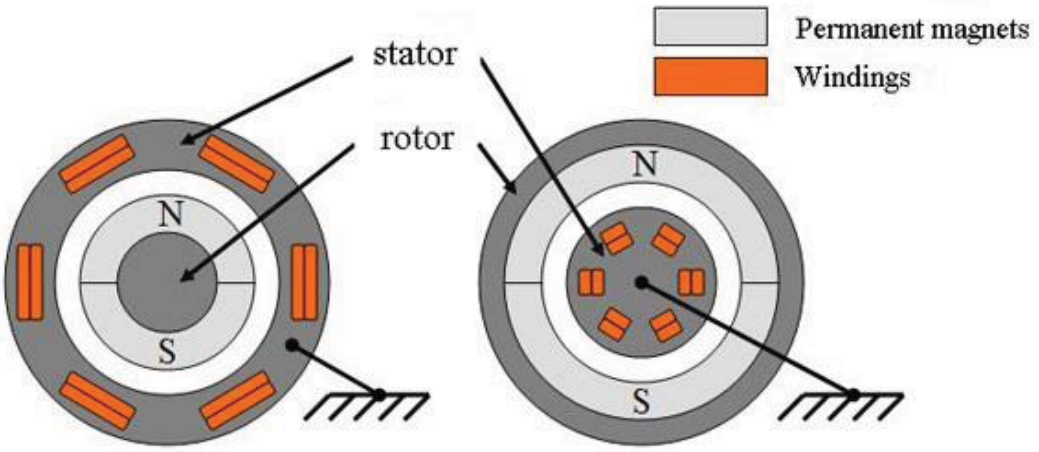

Figure 1.2 – Comparison of internal and external permanent magnet synchronous motor constructions [9]

According to the construction of the PMSM rotor, permanent magnets can be mounted on the rotor surface (surface permanent magnet synchronous motor – *SPMSM*) or inside the rotor (interior permanent magnet synchronous motor – *IPMSM*), as shown at Fig. 1.3.

As magnetic permeability of air and permanent magnets is almost equal ($L_d = L_q$), in SPMSM electromagnetic system is symmetrical, which makes it a non-salient pole motor, in contrast to IPMSM). This type of rotor construction allows to easily implement a control system. Since inductances along the transverse and longitudinal axes are almost equal, the motor torque is directly proportional to the i_q current component.

Motors with interior magnets are more reliable and robust, which allows them to be operated at higher speeds [10]. Since their electromechanical system is asymmetrical, there is an additional reactive torque component, which can be used to obtain greater torque/current ratios [11] and makes the motor suitable for loss-minimization control strategies, allows to decrease current during flux weakening operation [12]. The greater the difference between inductances L_d / L_q, the greater is reactive torque component and a wider speed range can be achieved.

The internal location of the permanent magnets allows to reduce the rotor diameter, which leads to total vehicle inertia reduction and, consequently, better dynamic performance. Implementation of this rotor structure also makes it possible to reduce vibrations during operation and increase the lifecycle of bearings.

SPMSM are used in low-power electric drives because of their cheapness and ease of production, but their disadvantages do not allow them to be used in mass electric vehicle production. IPMSM is preferred for electric vehicle applications, whereas its higher initial cost can be compensated during operation by higher energy efficiency. And the main advantage of the motors with the internal location of the permanent magnets is the ability to utilize flux-weakening control methods, which makes it possible to extend speed range.

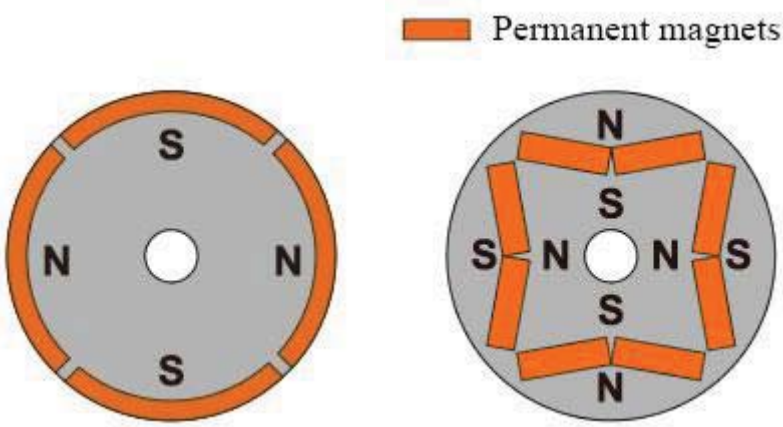

Figure 1.3 – Comparison of surface and interior permanent magnet synchronous motor constructions [9]

In comparison with IM and DC motors, the main advantages of PMSM are the following [13-15]:

- *High energy efficiency*. The use of permanent magnets does not require an additional energy source to create a magnetic field. The absence of a commutator and brushes reduces mechanical friction losses.

- *Good mass-dimensional characteristics*. The use of permanent magnets allows creating a magnetic flux with high density. This makes it possible to produce higher torque, and therefore, to decrease motor weight.
- *Ease of control*. The machine parameters practically do not depend on external influences and can be easily identified. The working principle of PMSM is similar to DC motor, control methods are simpler than algorithms for induction motor.
- *Efficient cooling*. The use of laminated steel and the absence of rotor windings reduces the heating of the rotor almost to zero. The main part of PMSM energy losses is caused by stator windings heating while cooling for this part of the motor is easier to realize. As a result, overload capacity $T_{\max} / T_{nom} = \{2...3\}$, and for air/water cooling machines $T_{\max} / T_{nom} = \{3...4\}$.
- *Low maintenance cost*. Because of the absence of a commutator and brushes, the machine requires no maintenance during all operation period. The reliability of the electromechanical system is determined by the winding insulation and bearings.
- *Low noise*. There is no noise from mechanical switching parts, and the switching frequency of the inverter transistors cab be set higher than the human threshold of hearing.

At the same time, PMSM has some disadvantages, the main ones are [16]:

- *Cost*. The construction of the stator is similar to an induction motor, so stator production costs are the same. However, the cost of rare-earth permanent magnets is high, and this significantly affects the final cost of the motor.
- *Demagnetization of permanent magnets*. Operation in high temperatures and demagnetization fields can cause magnetic properties deterioration.
- *Limited maximum speed*. The surface location of the permanent magnets prevents the rotor from operating at high speeds.

- *Narrow constant power region.* Due to provided constant magnetic flux by permanent magnets, SPSM has a relatively narrow constant power operation range. However, this problem can be solved by the appropriate control algorithm usage.

1.3 Overview of PMSM control algorithms

Today, the most common PMSM control strategies, used in the automotive industry, can be divided into scalar and vector.

In the *scalar control* method, only the magnitude of voltage is changing proportionally to the frequency, and not the position of the vector. This control algorithm can be used only in steady-state operation modes, because during transition processes it is not constant, which leads to torque and speed fluctuations.

Vector control techniques allow to independently change the motor flux and torque using the stator current components in the same way as flux and torque are regulated in Separately Excited DC motor. Firstly developed for IM by F. Blaschke in 1971 [17], vector control is also used for PMSM. It allows increasing system performance by providing high accuracy, a wide speed range, fast response, and reduced losses [18]. Widespread practical implementation of vector control began after the development of semiconductor devices and now is of great interest.

These methods don't have the disadvantages of scalar control but are much more complicated since they require more sensors, increased measurement accuracy, and a significant number of real-time calculations. Besides, parameters variation can be a significant problem for these algorithms.

The most popular vector control strategies of PMSM are Field Oriented Control (*FOC*), Direct Torque Control (*DTC*), and Field-weakening Control (*FWC*).

Field Oriented Control, often named $i_d = 0$ control, makes it possible to control motor flux and torque independently. By adjusting the direct axis component equal to zero, it keeps the permanent magnet magnetic field in the direction of the d-axis. This leads to the linear relationship between torque and q-axis current

component. FOC is a common control strategy for SPMSM, however, it not so efficient for IPMSM because does not allow to use of reactive torque component.

Direct Torque Control was introduced in 1985 as an attempt to overcome *FOC* shortcomings, which were: high complexity of computational algorithms and significant dependence on measurement and calculation accuracy.

Since stator flux and electromagnetic torque are controlled directly and there is no need for coordinate system transformation, this algorithm is easier to implement and provides better torque response. Also, it is robust for parameter variations.

Field-weakening control allows expanding speed range. When the motor voltage reaches the inverter's limit, the current regulator is saturated. For operation above rated speed, flux-weakening control strategies have to be used. Its working principle is the same as in Separately Excited DC motor: exciting current reduction makes it possible to reach higher rotational speed. Should be mentioned that in PMSM field cannot be weakened directly since the rotor field is produced by permanent magnets; d-axis armature reaction is used.

Nowadays of great interest are optimal control strategies based on vector control algorithms. Currently, the task of the optimal control in the electric vehicle industry is loss minimization. The most widely used optimal control algorithms are maximum torque per ampere (*MTPA*), maximum torque per volt (*MTPV*), loss minimization algorithm.

These control algorithms are used in different speed ranges: MTPA is used under the rated speed (most of the losses are caused by the stator winding heating) and MTPV above the rated speed (most of the losses are caused by supply voltage increasing).

1.4 Permanent magnets

Technology advancement and price reduction over the past few years made permanent magnets in high demand for almost all types of applications, from

household equipment to electric vehicles. In general, three types of PM are currently used for electric motors [16]:

- Alnico (aluminum-nickel) (Al, Ni, Co, Fe);
- Ceramic (ferrite), for example, barium ferrite (BaO × 6Fe2O3) and strontium ferrite (SrO × 6Fe2O3);
- Rare-earth materials: samarium-cobalt (SmCo) and neodymium-iron-boron (NdFeB).

The main advantages of *Alnico* are high flux density and low-temperature coefficient. These advantages make it possible to provide a high flux density in the air at high temperatures. However, their demagnetization curves are nonlinear. Thus, Alnico magnets are easy not only to magnetize but also to demagnetize. Alnico magnets are used in motors ranging from a few watts to 150 kW. Alnico was widespread in the industry until 1970 when ferrite-based magnets became more popular.

Barium and strontium *ferrites* were created in the 1950s. Ferrite has a higher coercive force than Alnico, but at the same time has a lower residual magnetic induction. The maximum operating temperature is 400ºC. The main advantages of ferrites are their low cost and very high electrical resistance, which leads to the absence of eddy currents.

Over the past three decades, the development of *rare-earth* magnets made it possible to achieve higher flux densities. The first generation of rare-earth PMs based on samarium-cobalt (SmCo5) was invented in the 1960s. SmCo5 offers high flux density, linear demagnetization curve, and low-temperature coefficient. The maximum operating temperature is 250-300ºC. Usage of these magnets allows the production of electric motors with the high power density and low inertia, however is quite expensive because of their rarity. The recent development of the second generation of rare-earth magnets based on neodymium (Nd) and iron (Fe) resulted in serious price reduction. NdFeB magnets have better magnetic properties than SmCo, but their demagnetization curves greatly depend on temperature.

1.5 Energy storage systems

The selection of an energy storage system is an important step in electric vehicle design since the power reserve and performance of the automobile directly depend on it. Up to now, the most commonly used energy storage systems for electric vehicles are batteries, fuel cells, and ultracapacitors.

Batteries are the most widespread type of energy storage system, used from the beginning of 1860. Electricity is stored in the form of chemical energy and provided to the electric drive through a process of electromechanical reaction when needed [19]. Due to low resistance, high power density, and a wide range of working temperatures, batteries are suitable for electric vehicle applications. But it must be taken into account that toxic materials are used for energy storage in batteries, the production of which can be harmful to the environment.

Batteries are combined in battery packs to obtain the desired current and voltage values, needed for the propulsion system of the vehicle. The main parameters that have to be considered when choosing a battery pack for electric vehicle application are the following [20]:

- Battery capacity;
- The voltage of a single element;
- Maximum charge / discharge current;
- Specific energy consumption;
- Energy density;
- Specific power;
- Life cycle;
- State-of-charge (*SOC*);
- Self-discharge rate;

In electric vehicles, the most used are the following types of batteries:

Lead-acid (LA) batteries have high rated voltage (2 V), low impedance, and relatively high efficiency (up to 85%) [21]. However, short life cycles, insufficient

strength, and bad performance at peak temperatures prevent them from widespread usage.

Nickel-metal hydride (NiMH) offers better characteristics than LA: they are stronger, unresponsive to overloads, have a wider range of operating temperatures, and can be used in harsh conditions. Nevertheless, their shortcomings are lower efficiency (up to 66%) and relatively low rated voltage (1.2- 1.33 V) [22].

Lithium-ion batteries (Li-Ion) are widely used in electronics and, especially, the automotive industry as energy storage systems for EV application. Their advantages are high energy density and low self-discharge [23].

The parameters of Li-Ion batteries greatly depend on the chemical composition:

- The voltage of a single element: 3.7 V;
- Specific energy consumption: 100… 200 W · h / kg;
- Operating temperature range: from -20 °C to +60 °C

Li-ion batteries have the best protection of all types. Usually, there are several options to implement it: field-effect transistor, which opens when element voltage reaches set limit; thermal fuse which opens the circuit in a case of overheat; deep discharge protection.

Lithium-phosphate (LiFePO4) batteries are a type of lithium-ion battery in which LiFePO4 is used as the cathode. The main advantages of these batteries are a longer lifecycle, stable discharge voltage, a wider range of operating temperatures, and safer operation [24].

Fuel cells (FC) are the type of energy storage systems that converts the chemical energy of stored fuel into electricity. Unlike batteries, the energy source for FC is supplied externally, which allows generating electric energy continuously as long as fuel is provided to the cell. The most popular are FC, based on Hydrogen, which generates electrical energy by combining hydrogen and oxygen [25].

Ultracapacitors are very similar in design to conventional capacitors, but they have a much larger capacitance and lower-rated voltage. The capacity of modern ultracapacitors is 1-10 F at a rated voltage of 3-4 V [26]. The main advantages of

ultracapacitors are as follows: fast charging time (just a few seconds), a big number of charge cycles (up to one million), better efficiency at peak temperatures. But their disadvantages are significantly lower specific power and energy consumption.

1.6 Requirements for electric vehicle drivetrains

Electric vehicle drivetrain scheme and elements selection is performed to provide the required performance. Parameters of the electromechanical system mustn't exceed maximum voltage and current. It is also necessary to take into account the driving cycle: high rate of acceleration, wide speed range, braking, and, especially in urban conditions, frequent start/stops. Also, regenerative braking must be used to increase efficiency, charging the battery via the kinetic energy of the vehicle. The energy source with the highest power density must be chosen, providing reduce battery size and increased vehicle power reserve [27,28].

In general, requirements for electric vehicle drivetrains can be divided into 4 groups: functional, constructional, operational, and economic [29].

One of the main *functional requirements* is a good dynamic performance. The traction motor has to be selected following the driving profile of the vehicle. Maximum efficiency over a wide speed range and high power density are necessary for traction motors to reduce total vehicle weight. Also, motors have to be able to be operated in tough conditions, such as high temperatures, humidity, and vibrations. Additionally, motors should have fast torque response, low acoustic noise, and high reliability.

Constructional requirements are the following: the weight of the traction motor should not be greater than 5-6% of the total vehicle mass. For IPMSM, permanent magnets should be installed in the rotor in such a way to obtain the desired ratio of direct and quadrature inductances, which can increase reactive torque components [30]. All elements of the electromechanical system should be protected against moisture and dust.

Operational requirements are the following: electric drive system should be able to work over a wide range of ambient temperatures (approximately from -40 °C to + 40 °C).

Economic requirements are the following: the cost of EV powertrain should not be more than 15-20% of the total vehicle cost, reasonable maintenance cost [31].

Chapter conclusions

Electric vehicles have significant advantages over conventional internal combustion cars. The rapid technological advancement has made electric vehicles a hot research area.

Main drivetrain elements were considered. It was shown that an interior permanent magnet synchronous motor can be used as a traction motor, providing high efficiency and great mass-dimensional characteristics.

Based on the analysis of energy storage systems, Li-ion batteries are selected.

Requirements for electric vehicle drivetrains were determined. Modern traction motor has to be selected by driving profile of the vehicle to provide maximum efficiency over a wide speed of range. Electric drivetrain should be able to work in harsh conditions, such as high temperatures, humidity, and vibrations.

CHAPTER 2. TRACTION MOTOR AND BATTERY PACK CALCULATION

According to [32], 91% of the world population live in places where the Air Quality Index (AQI) exceeds World Health Organization limits. The transport industry is one of the biggest sources of air pollution, especially in big cities, because of internal combustion engine usage. As electric vehicles can be a solution to this problem, in this thesis conventional car with an internal combustion engine is converted into PMSM-driven electric vehicle. It was decided to take Mini Countryman 1.5 MT One [33] as the basis car, as this compact vehicle is perfect for city usage. The main parameters of the vehicle [34] are shown in Table 2.1.

Figure 2.1 - Mini Countryman 1.5 MT One [33]

Table 2.1 – The main parameters of the vehicle

Vehicle mass	$m = 1440\ kg$
Vehicle frontal area	$S = 1.83\ m^2$
Rolling resistance coefficient	$f = 0.01$
Aerodynamic drag coefficient	$C_x = 0.32$
Wheel radius	$R = 0.3\ m$
Reduction gear ratio	$i = 3$

2.1 Driving cycle creation

Firstly, the desired performance characteristics of the automobile should be defined. Let us consider vehicle acceleration speed from 0 to 100 *km/h* equal to 10 *s* and top speed equal to 140 *km/h*. Then, vehicle acceleration is given by:

$$a = \frac{100km/h}{10s} = \frac{27.8m/s}{10s} = 2.78\left(\frac{m}{s^2}\right). \tag{2.1}$$

Maximum wheel angular speed is given by:

$$v_{\max} = \omega_w \cdot r_w, \tag{2.2}$$

$$\omega_w = \frac{v_{\max}}{r_w} = \frac{140km/h}{0.3m} = \frac{38.8m/s}{0.3m} = 129.3\left(\frac{rad}{s}\right), \tag{2.3}$$

where $v_{\max}$ is the vehicle's top speed, ω_w is the wheel angular velocity, r_w is the radius of the wheel. Converting *rad/s* into *rpm*, we obtain:

$$n_w = \omega_w \cdot \frac{30}{\pi} = 129.3rad/s \cdot \frac{30}{\pi} = 1235.3\ (rpm), \tag{2.4}$$

where n_w is the wheel angular velocity in *rpm*.

The power reserve of the electric vehicle is taken equal to 160 *km*, as it is enough for city usage in Ukraine. For further calculations, it is considered that the driving cycle is equal to 40 km, representing 25% of vehicle power reserve. The selected driving cycle simulates the vehicle movement, consisting of frequent start/stops and two regions of acceleration from zero to top speed. It is shown in Fig. 2.2.

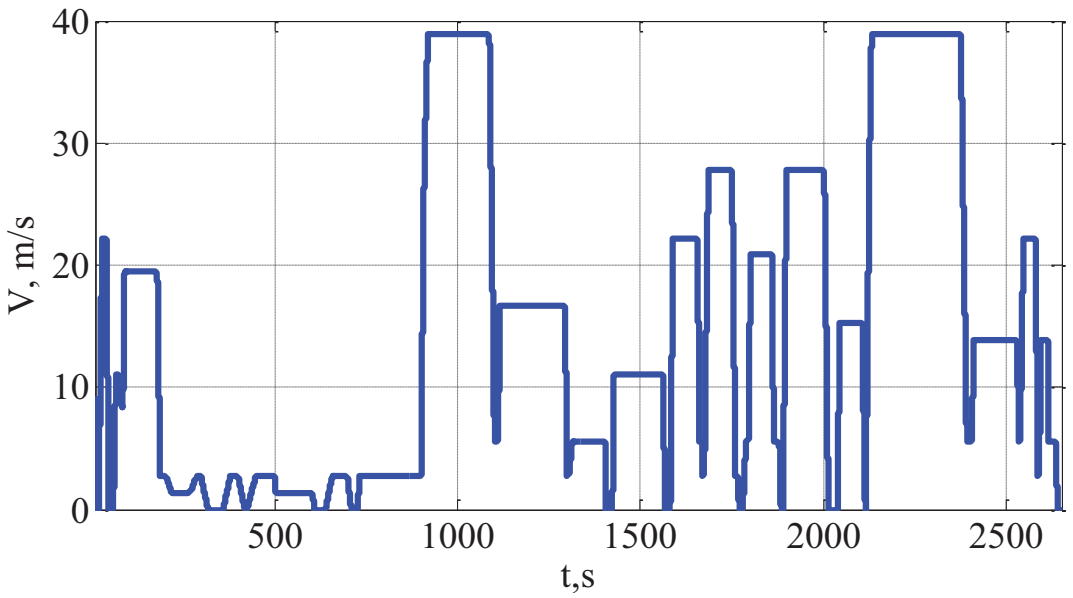

Figure 2.2 – Driving cycle

Distance *S*, which vehicle covers during one driving cycle, can be computed by the integration of velocity function, as follows:

$$S = \int v(t)dt. \tag{2.5}$$

Acceleration is the first derivative of the velocity function:

$$a(t) = \frac{dv}{dt}. \tag{2.6}$$

Distance and acceleration during one driving cycle are shown in Fig. 2.3 and Fig. 2.4, respectively.

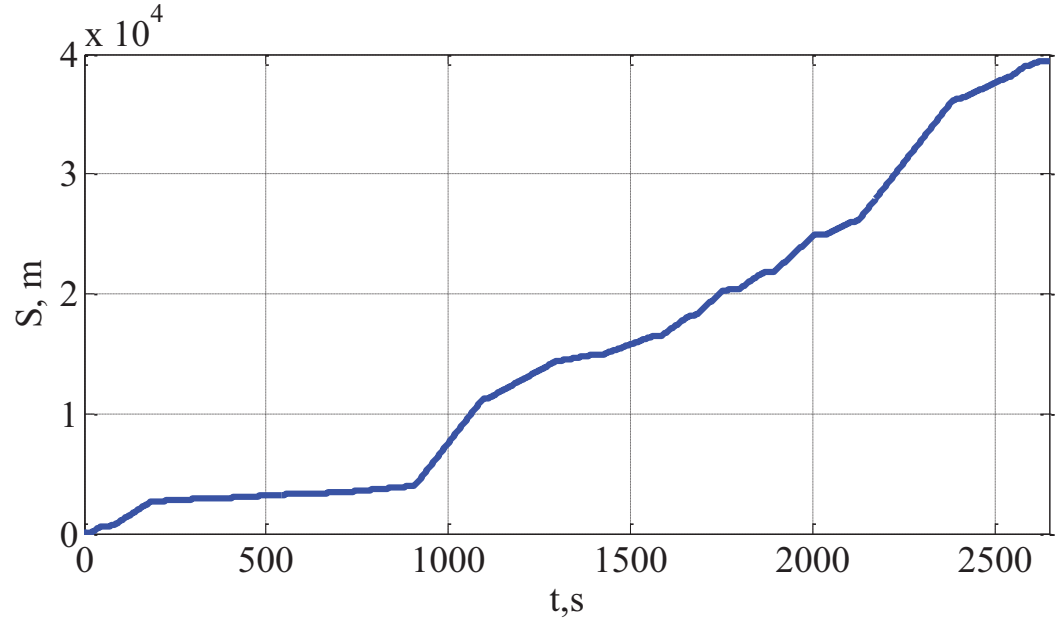

Figure 2.3 – Distance, covered during one driving cycle

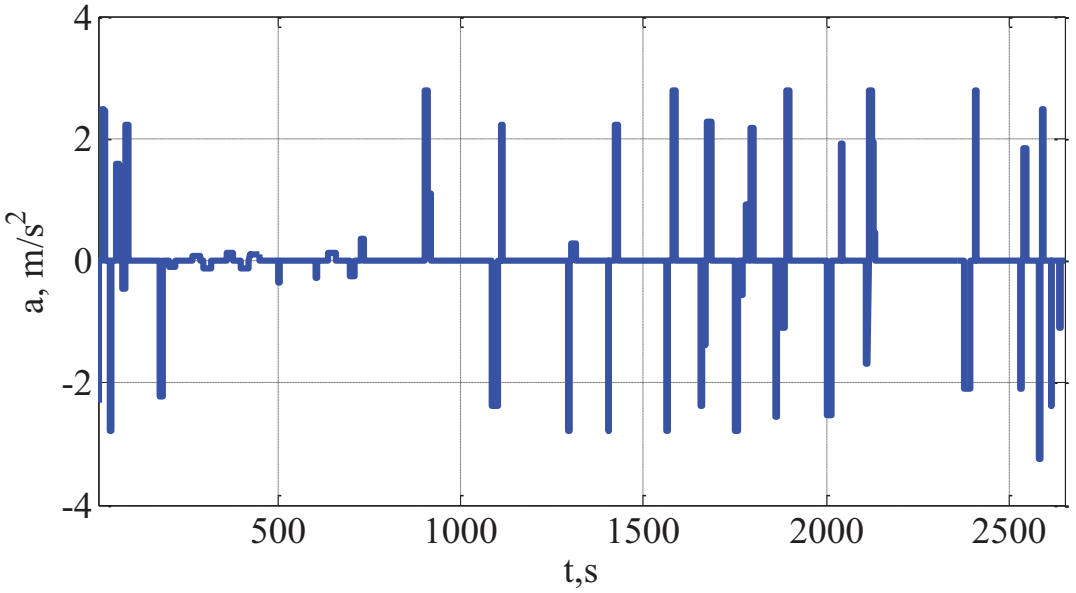

Figure 2.4 – Acceleration of the vehicle during the driving cycle

As can be seen in Figs. 2.3 and 2.4, the path covered in one drive cycle is equal to 40 *km*, representing 25% of vehicle power reserve, and vehicle acceleration doesn't exceed maximal calculated value.

2.2 Traction motor calculation

To simulate vehicle performance, motion equations have to be obtained. It can be done by analyzing all forces, acting on the vehicle during its motion. For the mathematical representation of the vehicle, a simplified model is used and shown in Fig. 2.5. Only forces of the movement along the longitudinal and vertical axes are considered [35].

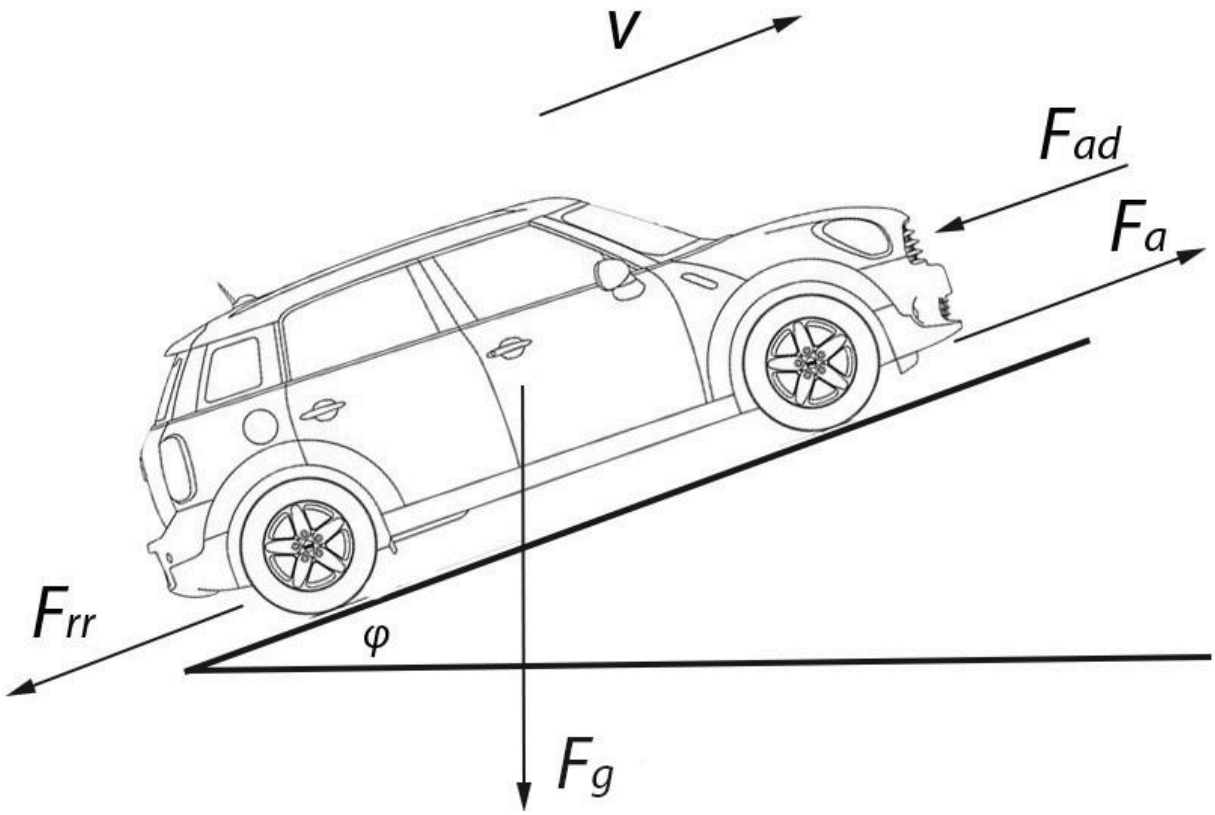

Figure 2.5 – Mechanical forces, that act on the vehicle

Force, propelling the vehicle forward, is called tractive effort F_T [36]. It includes both static and dynamic components, and can be calculated by the following formula:

$$F_T = F_{rr} + F_{ad} + F_g + F_a, \tag{2.7}$$

where F_{rr} is the rolling resistance force, F_{ad} is the aerodynamic drag, F_g is the grade resistance, F_a is the acceleration force. If provided traction power is big

enough to overcome the listed above resistance forces, the vehicle will propel forward.

The rolling resistance force is a result of the vehicle tire and the road surface contact. It doesn't depend on the vehicle speed and can be assumed constant. The equation that describes the rolling resistance force is as follows:

$$F_{rr} = fmg\cos\varphi \tag{2.8}$$

where f is the rolling resistance coefficient, m is the vehicle mass, g is the acceleration of gravity, φ is the road slope. For simplicity, in this thesis, the road slope is considered to be equal to zero ($\cos\varphi = 1$).

The rolling resistance force results in:

$$F_{rr} = fmg\cos\varphi = 0.01 \cdot 1440kg \cdot 9.81m/s^2 = 141.3\ (N). \tag{2.9}$$

Aerodynamic drag depends on the air density ρ, the aerodynamic drag coefficient C_x, the vehicle frontal area S, and vehicle speed v, as follows:

$$F_{ad} = 0.5C_xS\rho v^2, \tag{2.10}$$

Since this force depends on the velocity, it will vary during the simulation of the driving cycle. For this purpose, let us consider the aerodynamic drag coefficient $k_{ad} = 0.5C_xS\rho v^2$, which is equal to:

$$k_{ad} = 0.5C_xS\rho = 0.5 \cdot 0.32 \cdot 1.83m^2 \cdot 1.29kg/m^3 = 0.38\left(\frac{kg}{m}\right). \tag{2.11}$$

Grade resistance occurs when the vehicle is moving up a slope. It is defined by:

$$F_g = mg\sin\varphi. \tag{2.12}$$

Assuming the road slope is zero, the grade resistance is also equal to zero.

Acceleration force is needed to accelerate the vehicle. It is described by Newton's second law:

$$F_a = ma, \tag{2.13}$$

Total simulated tractive effort is shown in Fig. 2.6.

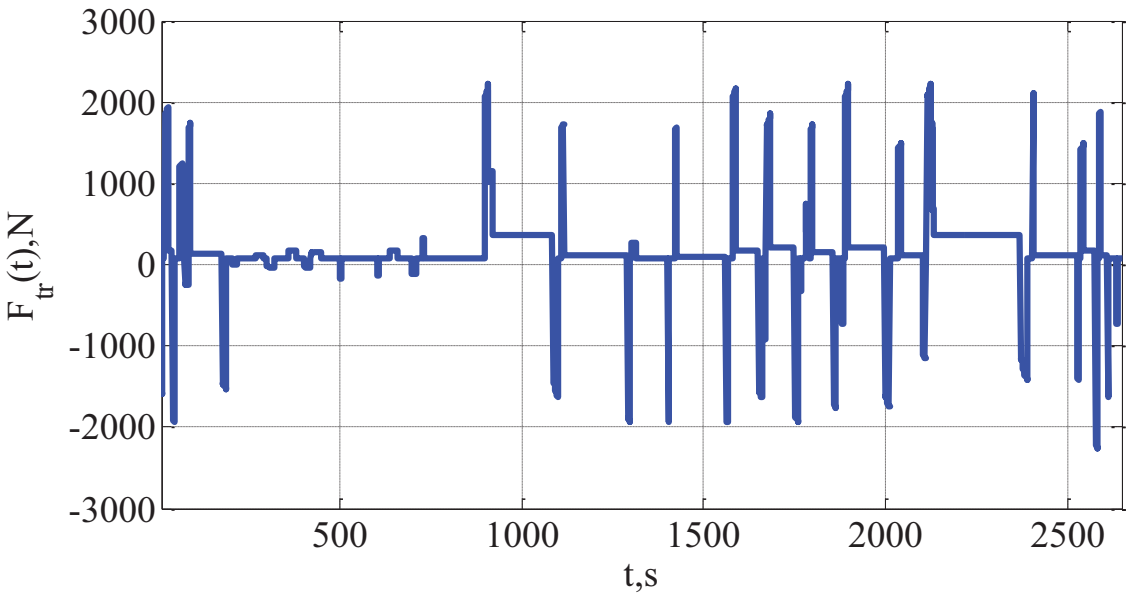

Figure 2.6 – Tractive effort of the vehicle during the driving cycle

Torque, which has to be produced by the traction motor, is given by:

$$T_m = \frac{F_T \cdot r_w}{i}, \tag{2.14}$$

where i is the reduction gear ratio.

From (2.14), the torque graph during the driving cycle was obtained. It is shown in Fig. 2.7.

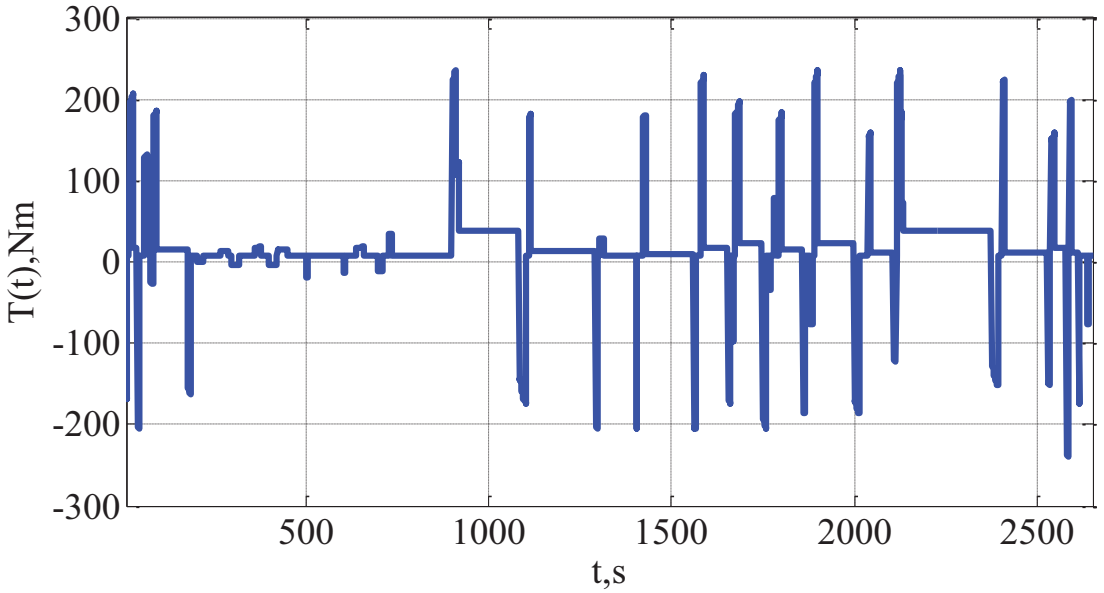

Figure 2.7 – Motor torque during the driving cycle

For further calculations, equivalent torque should be known. It is calculated via numerical integration of torque function $T(t)$, given in Fig. 2.7. The equation that describes it is as follows:

$$T_{equiv} = \sqrt{\frac{1}{t_{drc}} \int_0^{t_{drc}} T_m^2(t)dt}, \tag{2.15}$$

where t_{dc} is driving cycle time.

From the above expression (2.15), it follows:

$$T_{equiv} = 59.16 \ (Nm). \tag{2.16}$$

The maximal angular rotational speed of the motor can be computed by the following equation:

$$\omega_{\max} = \frac{v_{\max} \cdot i}{r} = \frac{38.9m/s \cdot 3}{0.3m} = 389 \ (rad/s). \tag{2.17}$$

Power, which motor has to produce to propel the vehicle forward during the selected driving cycle, is described by:

$$P_m = k_s T_{equiv} \omega_n, \tag{2.18}$$

where $k_s = 1.1 \div 1.3$ is the safety factor, ω_r is the motor rated angular speed.

Let us assume that vehicle rated linear speed is 100 *km/h*, or 27.8 *m/s*. Then, the rated angular speed of the traction motor is given by:

$$\omega_r = \frac{v_{vr} \cdot i}{r_w} = \frac{27.8m/s \cdot 3}{0.3m} = 278 \left(\frac{rad}{s} \right), \tag{2.19}$$

Now the traction motor power, which satisfies the chosen driving cycle, can be calculated according to (2.18):

$$P_m = 1.2 \cdot 59.16Nm \cdot 278rad/s = 19.7 \ (kW). \tag{2.20}$$

PMSM is selected by the calculations above. Its parameters are shown in Table 2.2.

Table 2.2 – Motor parameters

Nominal power	21 *kW*
Maximum rotational speed	6000 *rpm*
Rated rotational speed	1500 *rpm*
Rated torque	134 *Nm*
d-axis stator inductance	0.368 *mH*
q-axis stator inductance	1.227 *mH*
Efficiency	96%
Stator resistance	0.0342 *Ohm*
The flux of rotor permanent magnets	0.0856 *Wb*
Rated stator voltage	380 *V*
Number of pole pairs	4
Inertia	0.0473 kgm^2

The selected motor has been designed for electric vehicle application, providing high overload capacity and rotational speed.

2.3 Battery pack calculation

Battery power P_{bat}, needed for one driving cycle, is given by:

$$P_{bat} = \frac{P_{mot}}{\eta_{red} \cdot \eta_{inv} \cdot \eta_{mot}}, \tag{2.21}$$

where P_{mot} is the traction motor power, η_{red} is the reduction gear efficiency (which is equal to 1 in our case), η_{inv} is the inverter efficiency, η_{mot} is the traction motor efficiency.

Energy W_{bat}, needed for one driving cycle is given by:

$$W_{bat} = \int P_{bat}. \tag{2.22}$$

And total battery power, needed for the full range is given by:

$$P_{bat} = \frac{4 \cdot W_{bat}}{3600}. \tag{2.23}$$

The required battery power graph is shown in Fig. 2.7.

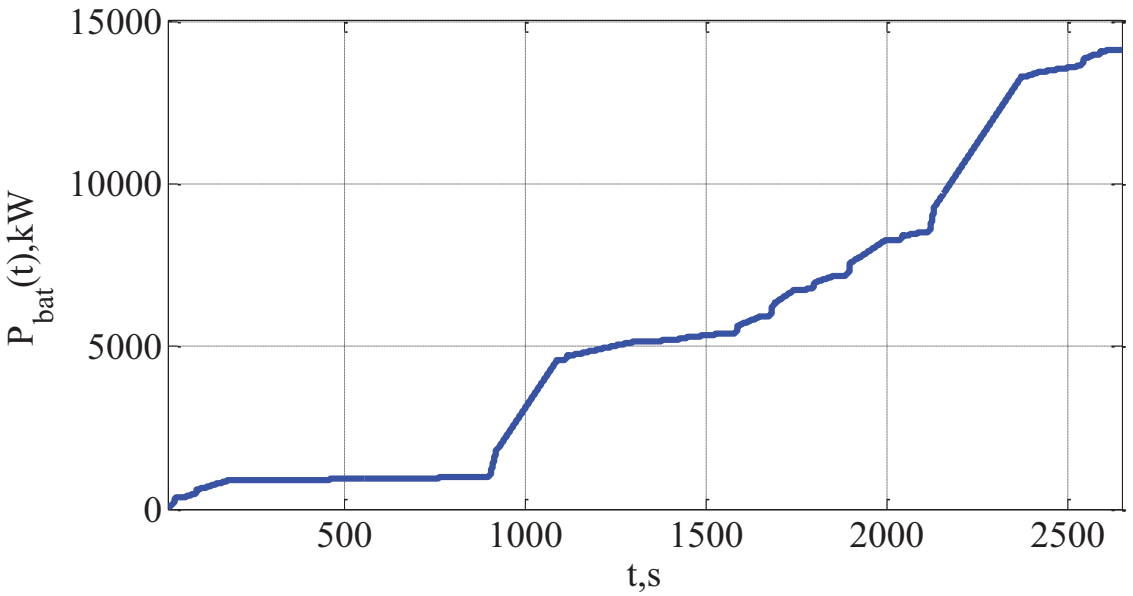

Figure 2.7 – Battery power graph

Battery voltage U_{bat} is given by:

$$U_{bat} = U_{ml} \cdot \sqrt{2} = 380V \cdot \sqrt{2} = 540 \ (V), \tag{2.24}$$

where U_{ml} is the line voltage of the motor.

Battery current is given by:

$$I_{bat} = \frac{P_{bat}}{U_{bat}} = \frac{14110W}{540V} = 26.13 \ (A). \tag{2.25}$$

To create a battery pack, GIF 18650 3.7V 9800mAh [13] cells are used.

The battery of the electric vehicle consists of several modules, connected in parallel. To create the required voltage, in one module have to be grouped the following number of cells, connected in series:

$$N_{cellsm} = \frac{U_{bat}}{U_{bat1}} = \frac{540V}{3.7V} = 146, \tag{2.26}$$

where U_{bat1} is the voltage of one battery cell.

The number of modules is given by:

$$N_{\mathrm{mod}} = \frac{I_{bat}}{I_{bat1}} = \frac{26.13A}{9.8A} = 3. \tag{2.27}$$

Hence, the total number of cells, used in the battery, is equal to

$$N_{cells} = N_{cellsm} \cdot N_{\mathrm{mod}} = 146 \cdot 3 = 438. \tag{2.28}$$

Chapter conclusions

This chapter presents the method of calculating the parameters of traction motor and battery pack for electric vehicle drivetrain, based on a conventional automobile with an internal combustion engine. According to the chosen driving cycle and desired vehicle performance, the required equivalent torque of the traction motor and battery pack capacity were determined.

A 21kW interior permanent magnet synchronous motor was selected to propel the vehicle.

Based on the presented calculation method, the battery-pack capacity needed for the estimated power reserve was chosen.

CHAPTER 3. PARAMETERS CALCULATION OF ELECTRIC VEHICLE DRIVETRAIN ELEMENTS

3.1 Power circuit

In electric vehicles, IGBT-based inverters are used to provide the required voltage to the traction motor. The electric drive block diagram is given in Appendix 1.

Rated phase voltage and current are given by:

$$U_r = \frac{U_{1r}}{\sqrt{3}} = \frac{380V}{\sqrt{3}} = 220\ (V), \tag{3.1}$$

$$I_r = \frac{P_2}{3U_r \eta \cos\varphi} = \frac{21000W}{3 \cdot 220V \cdot 0.97 \cdot 0.9} = 36.44\ (A), \tag{3.2}$$

where U_{1r} is rated line stator voltage, P_2 is traction motor power, η is motor efficiency, $\cos\varphi$ is power factor.

Peak voltage and current are defined by:

$$U_{rp} = \sqrt{2}U_r = \sqrt{2} \cdot 220V = 311\ (V), \tag{3.3}$$

$$I_{rp} = \sqrt{2}I_r = \sqrt{2} \cdot 36.44A = 51\ (A). \tag{3.4}$$

The maximum current in the motor winding is determined by electric drive overload capacity, which is equal to $k_{ovl} = 3 \div 5$ for vehicles. Let us consider $k_{ovl} = 4$, then:

$$I_{\max} = k_{ovl} I_{rp} = 4 \cdot 51A = 204\ (A). \tag{3.5}$$

When selecting IGBT for inverters, their maximal collector-emitter voltage has to be at least 1.5 times greater than the peak voltage of the DC-link. In electric vehicle powertrains, peak DC-link voltage is equal to battery voltage, which is $540V$ in our case.

$$U_{ce\min} = 1.5U_{dc\max} = 1.5 \cdot 540V = 810\ (V). \tag{3.6}$$

Two parameters have to be met when selecting IGBT:

$$I_{IGBT} > I_{\max},\ U_{IGBT} > U_{ce\min} \tag{3.7}$$

where I_{IGBT} is the collector current, U_{IGBT} is the collector-emitter voltage.

Based on the above calculations, the IGBT module Semikron SKiM459GD12E4 is selected [37]. The main parameters of the chosen module are shown in Table 3.1.

Table 3.1 – IGBT module parameters

Nominal collector current $I_{IGBT},\ A$	450
Peak collector-emitter voltage $U_{IGBT},\ V$	1200
Gate voltage $\Delta U_G,\ V$	-8…+15
Gate charge $Q_G,\ nC$	2550
Gate resistance $R_G,\ Ohm$	1.7

Gate drivers are used to generating control signals for IGBT and to provide electrical isolation (usually via optocouplers) between control and power circuits [38]. As can be seen from the selected IGBT module datasheet, the gate voltage is $\Delta U_G = (-8V ... + 5V)$, the gate charge is $Q_G = 2550nC$, gate resistance is $R_G = 1.7Ohm.$ Let us consider PWM switching frequency equal to $f_{sw} = 10kHz$. To select the appropriate gate driver, average and peak output currents have to be calculated, as follows:

$$I_{outav} = Q_G f_{sw} = 2550nC \cdot 10kHz = 25.5\ \left(mA\right), \tag{3.8}$$

$$I_{outp} = \frac{\Delta U_G}{R_G} = \frac{23V}{1.7Ohm} = 13.5\ \left(A\right). \tag{3.9}$$

Based on the calculated above gate driver parameters, Semikron SKYPER 12 press-fit 300A [39] is chosen, as it meets the following requirements:

$$I_{outpdriver} = 30A\ >\ 13.5A, \tag{3.10}$$

$$U_{cedriver} = 1200V > 810V, \tag{3.11}$$

$$Q_G = 50000nC > 2550nc, \tag{3.12}$$

$$f_{sw} = 30kHz > 10kHz. \tag{3.13}$$

DC-link capacitors are vital elements of the electric drive. They are used to minimize voltage and current fluctuations and to protect the subsystems of an electric vehicle from electromagnetic interference. The crucial aspect to choose the appropriate capacitor is the maximal battery current. It was decided to choose 3 film capacitors TDK B32678J1856K000 [40], connected in parallel. The main parameters of the capacitors are listed in Table 3.2.

Table 3.2 – DC-link capacitors parameters

Peak operating voltage U_{outp}, V	900
Peak current $I_{RMS\max}$, A	82.5
Capacitance C, μF	85

To ensure proper performance of electric drivetrain and to create current and voltage feedback loops, it is necessary to select current and voltage sensors.

The current sensors are selected according to the maximum measured current. As a current sensor, HAH3DR 700-S03/SP4 Hall-effect transducer [41] is chosen with the maximum measured current $I_{cs\max} = 700A > I_{dc}$. The main parameters of the sensor are shown in Table 3.3.

Table 3.3 – Current sensors parameters

Measuring range I_{PM}, A	±700
Output voltage U_{out}, V	0..5
Supply voltage U_c, V	+5

Voltage sensor LV-25NP [42] and resistor, connected in series, are used to measure DC-link voltage. The wiring diagram is illustrated in Fig. 3.1, while the main parameters are shown in Table 3.4.

Table 3.4 – Voltage transducer parameters

Measuring range I_{PM}, mA	$0..\pm 14$
Output current I_{out}, mA	0..25
Supply voltage U_c, V	±15

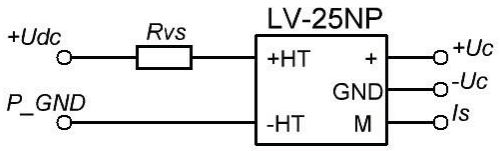

Figure 3.1 – Voltage transducer wiring diagram

As peak current in sensor primary circuit is $I_{p\max} = 14mA$ required resistance is given by:

$$R_{vs} = \frac{U_{dc\max}}{I_{p\max}} = \frac{540V}{0.014A} = 38571\ (Ohm). \quad (3.14)$$

From standard resistor values, resistor CF1/4W-39K [43] with value $R_{vs} = 39\ kOhm$ is chosen.

3.2 Control circuit

For the speed feedback loop, ELTRA EMI 55 encoder is chosen [44]. Its main parameters are given in Table 3.5.

Table 3.5 – Encoder parameters

Resolution, *ppr*	up to 2048
Peak load current for channel I_{load}, mA	15
Supply voltage U_c, V	+5
Max output frequency f_{out}, kHz	200

The wiring diagram is shown in Fig. 3.2, where *X1* is the terminal block with output signals from the encoder, U_1,U_2 are Texas Instruments LM393 comparators [45], $U_3 - U_5$ are 6N137 Vishay Semiconductors optocouplers [46], $R_1 - R_3$ are CF1/4W-47R resistors [43] with value 47 *Ohm*, $C_1 - C_5$ are CCK-100N capacitors [43] with value 100 *nF*. The main parameters of the optocouplers are given in Table 3.6.

Table 3.7 – Optocouplers parameters

Input current I_F, *mA*	30
Input reverse voltage U_R, *V*	5
Output current I_o, *mA*	50
Output voltage U_o, *V*	7

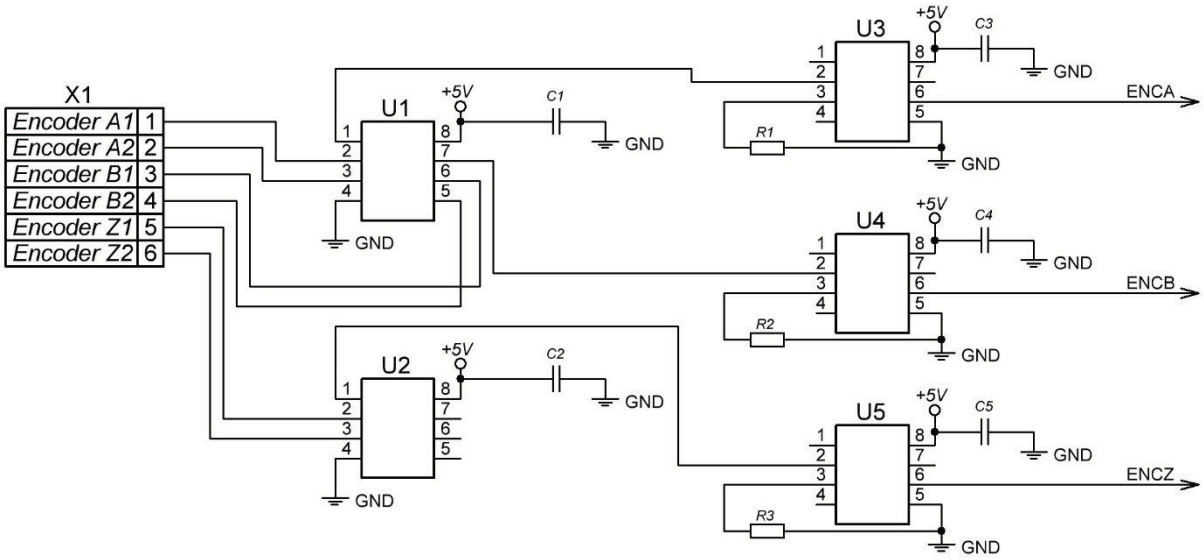

Figure 3.2 – Encoder wiring diagram

Digital signals processors are used to control real-time systems. 32-bit microcontroller (MCU) TMS320F28067 [47] is chosen as main system controller, since it is designed for high-speed closed loop performance in apllications such as electric vehicles. Main prarameters are shown in Table 3.8.

Table 3.8 – Microcontroller parameters

Clock speed f, *MHz*	90
Supply voltage U_c, *V*	3.3
RAM, *KB*	100
Flash, *KB*	256
Number of PWM channels, pcs	16
ADC	12-bit

Quartz crystal Oscilent 161-10.0M-20-25GP [48] is used to provide a stable reference oscillation signal, it is connected to *PIN47* and *PIN48* of MCU. Wiring diagram is presented at Fig. 3.3, where C_1, C_2 are CCK-33P capacitors [43] with value 33 *pF*.

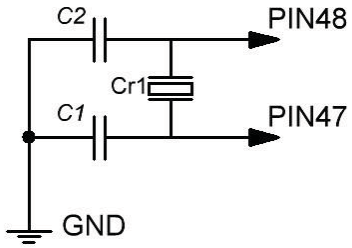

Figure 3.3 – Oscillator wiring diagram

It is necessary to provide stable power to MCU for its better operation. This is done with the help of TPS75333 voltage regulator [50] supplying +3.3*V* output voltage. To increase protection from interference, CCK-33P [33] filtering ceramic capacitors $C_1 - C_{11} = 100$ *nF* are chosen. For regulator connection, the following elements are used: CCK-33P [33] capacitors $C_{12}, C_{13} = 100$ *nF*, WL1E227M1012MBB [43] low-impedance capacitors $C_{14}, C_{15} = 220$ μF, 1.3W-20V [43] Zener diode *VD1*. Light-emission diode *HL1* is used for voltage presence indication, RESET turns off MCU automatically when supply voltage drops lower than 95% from rated. Wiring diagram is shown at Fig. 3.4.

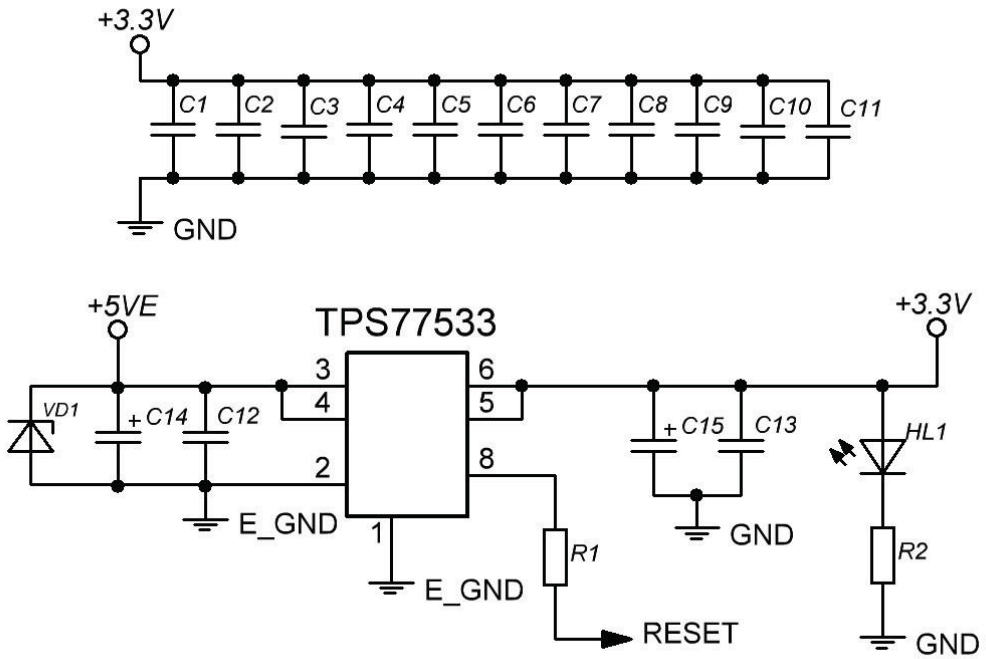

Figure 3.4 – Power supply wiring diagram

For data storage EEPROM AT250 [50] is connected via Serial Peripheral Interface (*SPI*), as shown at Fig. 3.5.

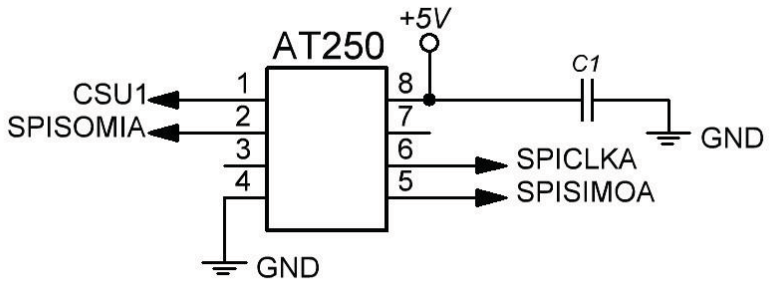

Figure 3.5 – EEPROM wiring diagram

As real-time clock (*RTC*), DS1305 [51] is selected and connected thtough *SPI*, as illustrated on Fig. 3.6. Quartz oscillator Abundance 32,768*kHz* is used for its proper operation.

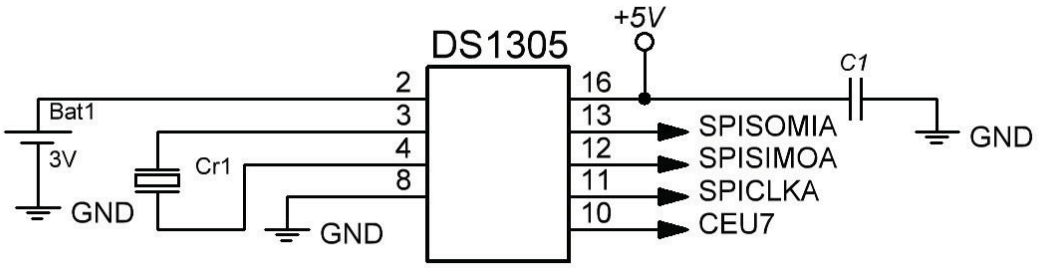

Figure 3.6 – RTC wiring diagram

Input signal from DC-link voltage transducer has to be scaled to acceptable MCU level before processing. This is done by signal conditioning circuit, as shown at Fig. 3.7.

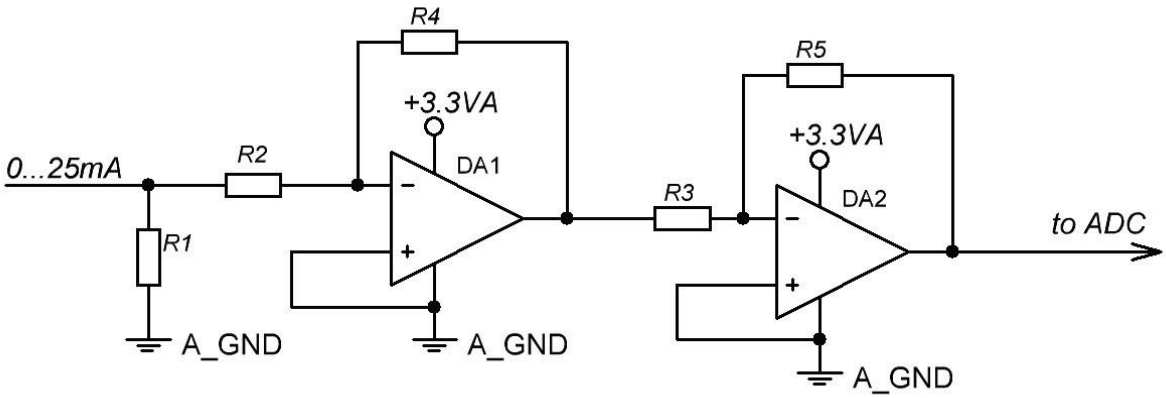

Figure 3.7 – DC-link voltage transducer signal conditioning circuit

Output signal of voltage transducer is $0...25\ mA$, then voltage across resistor is given by:

$$U_{R_1} = I_{out} R_1. \tag{3.15}$$

Thus, required resistance R_2 can be calculated by the following formula:

$$R_1 = \frac{\Delta U_{trans}}{I_{out\,\max}} = \frac{5V}{0.025A} = 200\ (Ohm). \tag{3.16}$$

Operational amplifier *DA1* (TL084) [52] gains and inverts input signal, then operational amplifier *DA2* inverts signal again to scale it to level acceptable to MCU

$U_{ADC\max} = 3.3\ V$. As output signal from sensor is unipolar, there is no need in additional signal shifting. Resistors $R_3 - R_5$ are selected equal to 10 *kOhm*, then:

$$R_2 = R_4 \frac{\Delta U_{trans}}{\Delta U_{ADC\max}} = 10^4\, Ohm \cdot \frac{5V}{3.3V} = 15\ (kOhm). \qquad (3.17)$$

Input signal from current sensor should be scaled in a similar way to voltage transducer, as illustrated on Fig. 3.8.

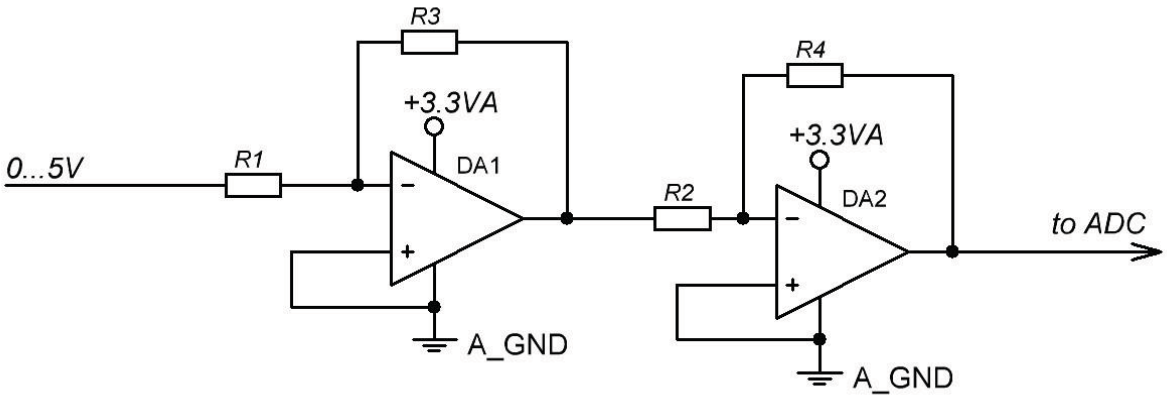

Figure 3.8 – Current sensor signal conditioning circuit

As output signal of current sensor is $0...5V$ there is no need in additional resistor at the circuit input.

3.3 Inputs and outputs

Analogue inputs realization is done in the same way as described above conditioning circuits, i.e. input signal should be scaled to meet MCU requirements. Taking into account that input analogue signal is $0...10\ V$ and assuming resistors $R_2 - R_4$ value is equal to 10 *kOhm*, we obtain:

$$R_1 = R_3 \frac{\Delta U_{in}}{\Delta U_{ADC\max}} = 10^4\, Ohm \cdot \frac{10V}{3.3V} = 30\ (kOhm). \qquad (3.18)$$

Analogue input signal electrical circuit is illustrated on Fig. 3.9.

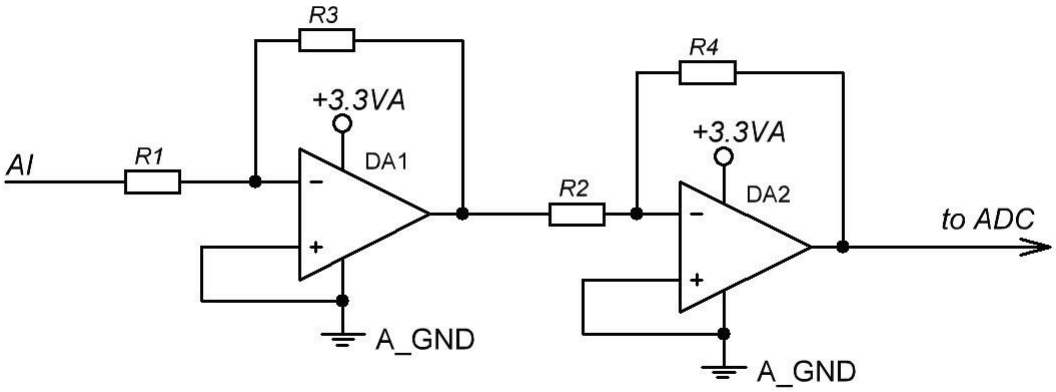

Figure 3.9 – Analogue input signal circuit

For $0...10\ V$ analogue output implementation, digital-to-analog converter (*DAC*) MAX5711 [53] and conditioning circuit are used, as shown at Fig. 3.10.

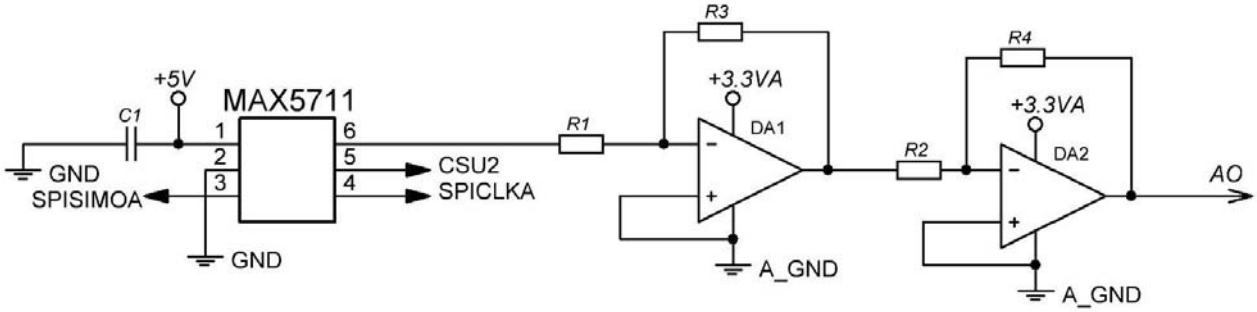

Figure 3.10 – Analogue output wiring diagram

Let us define $R_2 - R_4$ value is equal to 10 *kOhm*, then resistance R_1 can be calculated by the following formula:

$$R_1 = R_3 \frac{\Delta U_{ADC\max}}{\Delta U} = 10^4\, Ohm \cdot \frac{3.3V}{10V} = 3.3\ (kOhm). \qquad (3.19)$$

The circuit with optocoupler PC814 [54] is used for digital input implementation, as shown at Fig. 3.11. Optocoupler provides galvanic isolation of power and control circuits. Resistor CF1/4W-330R [43] with the value $R_1 = 330\ Ohm$ limits input current, while $R_2 = 10\ kOhm$ is a pull-up resistor 1/4W10K [43].

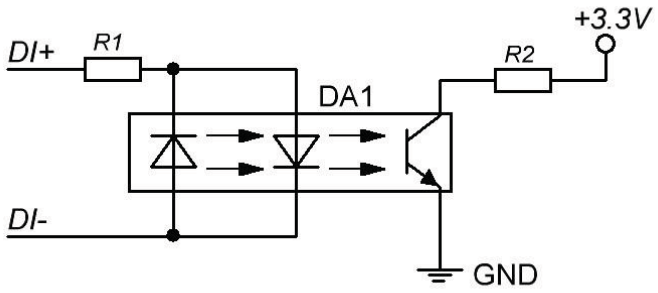

Figure 3.11 – Digital input signal circuit

Resistance R_1 can be calculated by the following formula:

$$R_1 = \frac{U_{in}}{I_{in}} = \frac{24V}{0.002A} = 1.2\ (kOhm). \tag{3.20}$$

From standard values, CF1/4W-1K2 [43] resistor is selected.

To match MCU *+3.3V* operating voltage and *+5V* output voltage, 74ACT540 (*U1*) [55] driver is used. To isolate control circuit, PC817 (*DA1*) [56] optocoupler is utilized. Wiring diagram is shown at Fig. 3.12. $R_1, R_2 = 1\ kOhm$ are pull-up resistors CF1/4W-1K [43].

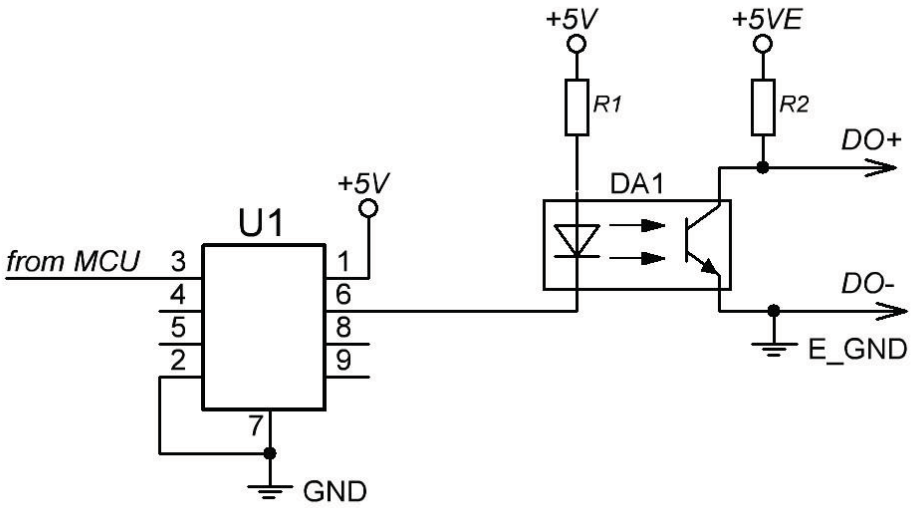

Figure 3.12 – Digital input signal circuit

Also, there are relay LEG5 on the scheme to configure dry contacts, as shown at Fig. 3.13. Relay dry contacts provide mechanical galvanic isolation, allowing to commutate high currents. These contacts are protected from noises, but their lifecycle is limited. Transistor *VT1* is used for signal amplification, while diode *VD1* is used for protection from current surges.

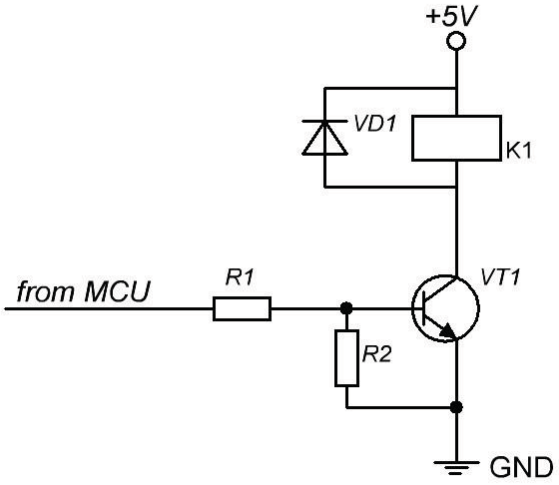

Figure 3.13 – Dry contact output

3.4 Communication ports

To implement connection through a CAN serial bus, transceiver ISO1050DUB (*U1*) [57] is used. Resistor CF1/4W-120R [43] with value $R_1 = 120\ Ohm$ is connected between output CAN signals. Connection diagram is given at Fig. 3.14.

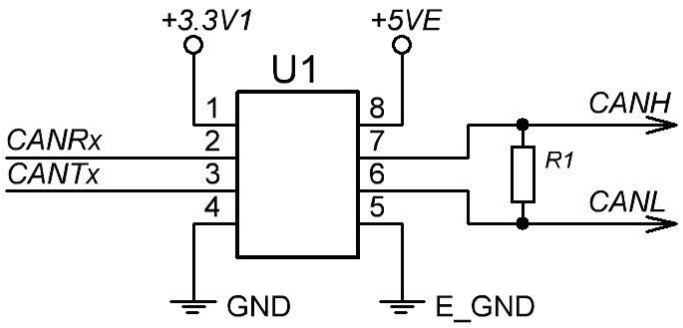

Figure 3.14 – CAN bus connection diagram

Communication port RS-485 is created with the help of MAX485 transceiver [58]. Resistor CF1/4W-120R [43] with value $R_2 = 120\ Ohm$ is connected between RS-485(A) and RS-485(B) signals, while $R_1, R_3 = 500\ Ohm$ are pull-down and pull-up resistors CF1/4W-510R [43], respectively. Connection diagram is shown at Fig. 3.15.

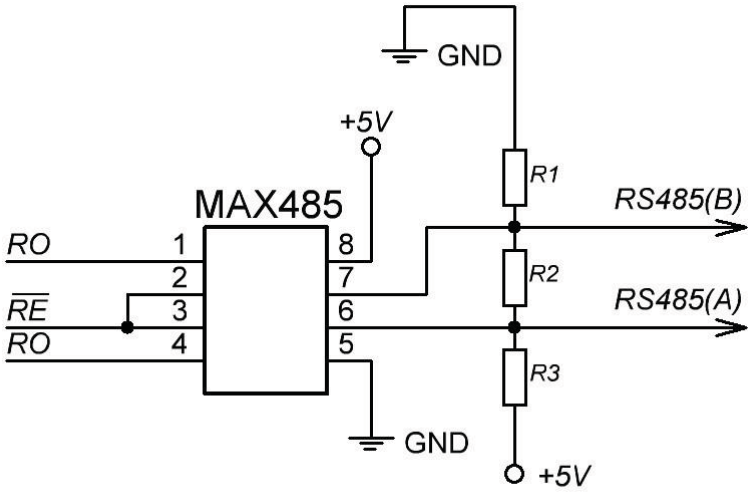

Figure 3.15 – RS-485 connection diagram

Chapter conclusions

In this chapter, electric vehicle drivetrain elements were selected. According to calculated traction motor power, IGBT-module, drivers, capacitors, current, and voltage transducers were chosen for the power circuit.

To operate the system, the microcontroller and its power supply were selected.

Conditioning circuits were developed to scale voltage and current sensors output signals to acceptable MCU level.

To create a speed feedback loop, an incremental encoder was chosen.

There were configured CAN and RS-485 interfaces with the help of transceivers.

CHAPTER 4. DEVELOPMENT OF LOSS MINIMIZATION CONTROL ALGORITHM OF IPMSM FOR ELECTRIC VEHICLE APPLICATION

Permanent magnet synchronous motor losses can be divided into mechanical, electrical, and additional. Mechanical losses can't be minimized via the control algorithm as they don't depend on mechanical rotor speed, however, it is possible to reduce them at the motor designing stage. Electrical losses can be divided into copper and iron and can be reduced with the help of a suitable control method

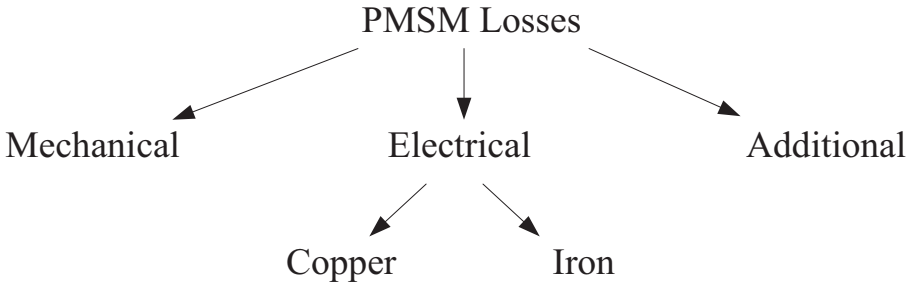

As there is no rotor winding in PMSM, copper losses can be calculated using the following equation [15]:

$$P_{Cu} = 3R_s I_s^2 = \frac{3}{2} R_s i_s^2 = \frac{3}{2} R i^2, \tag{4.1}$$

where $I_s = \frac{i_s}{\sqrt{2}}$.

Iron losses mostly consist of eddy current losses, as follows:

$$P_{Fe} = \frac{3}{2} k_{ec} \omega_e^2 \psi_m^2, \tag{4.2}$$

where $\psi_m = \frac{e_m}{\omega_e} = \sqrt{\psi_d^2 + \psi_q^2} = \sqrt{(\psi_{pm} + L_d i_d)^2 + (L_q i_q)^2}$.

Taking into account the fact that coordinate system rotation speed is equal to rotor electrical speed $\omega_k = \omega_e$, iron losses are given by:

$$P_{Fe} = \frac{3}{2} \cdot \frac{e_m^2}{R_{ec}} \approx \frac{3}{2} \cdot \frac{u_s^2}{R_{ec}}. \tag{4.3}$$

4.1 Mathematical model of the motor

To analyze IPMSM, a mathematical model in (d-q) coordinate system is used, which can be described by the following equations:

$$\begin{cases} u_d = Ri_d + L_d \dfrac{di_d}{dt} - \omega_e \psi_q, \\ u_q = Ri_q + L_q \dfrac{di_q}{dt} + \omega_e \psi_d, \\ T = k_t \left[\psi_{pm} i_q + (L_d - L_q) i_d i_q \right], \\ J \dfrac{d\omega}{dt} = T - T_L. \end{cases} \tag{4.4}$$

where

$$\omega_e = p\omega,\ \psi_q = L_q i_q,\ \psi_d = L_d i_d + \psi_{pm}. \tag{4.5}$$

Substituting/inserting (4.5) into (4.4), we obtain

$$\begin{cases} u_d = Ri_d + L_d \dfrac{di_d}{dt} - \omega_e L_q i_q, \\ u_q = Ri_q + L_q \dfrac{di_q}{dt} + \omega_e (L_d i_d + \psi_{pm}), \\ T = k_T \left[\psi_{pm} i_q + (L_d - L_q) i_d i_q \right], \\ J \dfrac{d\omega}{dt} = T - T_L. \end{cases} \tag{4.6}$$

where i_d, i_q are the stator current components, u_d, u_q are the stator voltage components, L_d, L_q are the direct and quadrature axis inductances of the stator, R is the stator winding resistance, ω, ω_e are the mechanical and electrical rotor angular speeds, p is the number of pole pairs, ψ is the permanent magnet rotor flux, J is the inertia of the rotor, T, T_L are the electromagnetic and load torques, $k_T = \dfrac{3}{2} p.$

Block diagram of IPMSM is shown in Fig. 4.1.

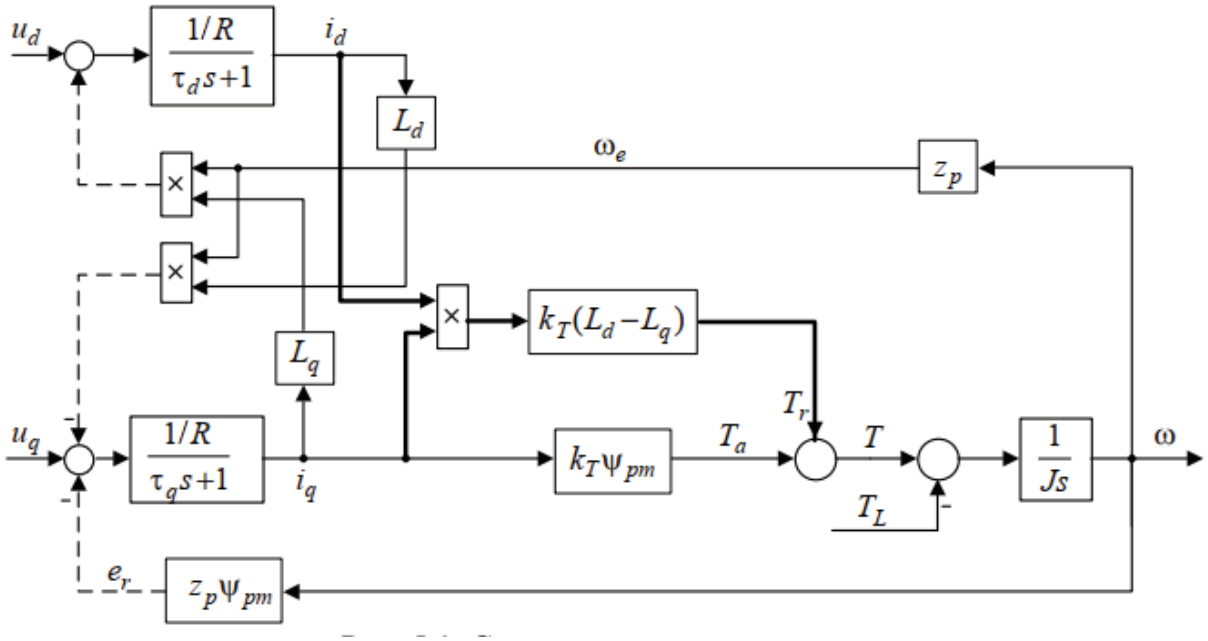

Figure 4.1 – IPMSM block diagram

As can be seen from (4.6), the torque equation consists of two components. Apart from the active torque component, $T_a = k_T \psi_{pm} i_q$, there is the reactive torque component $T_r = k_T (L_d - L_q) i_d i_q$, which is the result of the magnetic asymmetry of IPMSM. Should be mentioned, that in SPMSM reactive torque component is absent, since $L_d = L_q$. This is also true for classical vector control with $i_d = 0$. Thus, to increase efficiency, the d-axis current must be non-zero. Below are presented strategies to determine i_d the current component.

In recent years of great interest are speed control systems of electric vehicles (so-called cruise control systems). The goal of the control algorithm is to constantly regulate motor torque, thereby maintaining the given speed which can be set by the diver or control system (like in autonomous vehicles). Cruise control results in efficient battery usage consequently increasing the efficiency of the whole drivetrain [60].

The transfer function of the d-axis current component regulator is given by:

$$W_{crd}(p) = \frac{(T_d p + 1)R}{T_c p}, \tag{4.7}$$

where $T_d = \frac{L_d}{R}$ is d-axis time constant of the stator control circuit, T_c is the time constant of the open-loop current controller and can be defined as follows:

$$T_c = \frac{(2...4)}{f_{PWM}}, \tag{4.8}$$

where f_{PWM} is PWM frequency.

The transfer function of the d-axis current component regulator is defined by:

$$W_{crq}(p) = \frac{(T_q p + 1)R}{T_c p}, \tag{4.9}$$

where $T_q = \frac{L_q}{R}$ is the q-axis time constant of the stator control circuit

The transfer function of the speed controller is given by:

$$W_{sc}(p) = \frac{J}{k_T \psi_{pm} T_\omega}, \tag{4.10}$$

where is $T_\omega = 2T_c$.

4.2 Maximum torque per Ampere control strategy

The goal of maximum torque per Ampere control strategy is to find the appropriate i_d / i_q ratio which provides the minimal stator current at constant torque or maximal torque at given stator current in steady-state. This leads to the reduction of copper losses. The MTPA control algorithm is mostly used in the range of speeds below the rated.

This optimal control problem is one of the conditional extremum problems and can be solved by the Euler-Lagrange method [59]. The function which has to be minimized is the stator current expression, as follows:

$$f(i_d, i_q) = i_s^2 = i_d^2 + i_q^2 \to \min. \tag{4.11}$$

Another task of the optimization is to provide the required reference torque:

$$g(i_d, i_q) = T - C_m i_q - k_T (L_d - L_q) i_d i_q = 0. \tag{4.12}$$

Lagrange function is given by:

$$L(i_d, i_q, \lambda) = f + \lambda g = (i_d^2 + i_q^2) + \lambda\left[T - C_m i_q - k_T(L_d - L_q) i_d i_q\right]. \quad (4.13)$$

The Euler-Lagrange equation is defined by:

$$\begin{cases} \dfrac{\partial L}{\partial i_d} = 2i_d - \lambda k_T(L_d - L_q) i_q = 0, \\ \dfrac{\partial L}{\partial i_q} = 2i_q - \lambda C_m - \lambda k_T(L_d - L_q) i_d = 0. \end{cases} \quad (4.14)$$

Solving (4.14), we obtain the required optimal combination of stator currents:

$$i_d = -\frac{\psi_{PM} + \sqrt{\psi_{PM}^2 + 4(L_d - L_q)^2 i_q^2}}{2(L_d - L_q)}. \quad (4.15)$$

Substituting (4.15) into the moment equation (4.6), the optimal i_q reference, which depends on torque reference, is obtained:

$$i_q^4 + \frac{T\psi_{PM}}{k_T(L_d - L_q)} i_q - \left(\frac{T}{k_T(L_d - L_q)}\right)^2 = 0. \quad (4.16)$$

It is complicated to solve (4.16) analytically, therefore required q-axis current component can be calculated by the following formula [15]:

$$i_q = \frac{T}{k_T\left[\psi_{PM} + (L_d - L_q) i_d\right]}. \quad (4.17)$$

4.3 Maximum torque per Volt control strategy

The goal of the maximum torque per volt strategy is to find the appropriate i_d / i_q ratio, which provides the required torque at a minimum stator voltage and flux, or maximal torque at a given stator voltage in a steady state. This leads to the reduction of iron losses, which are proportional to u^2. Usually this algorithm is used for speeds higher than rated.

Let us define voltage equations without voltage drops at active and reactive resistances, as follows:

$$\begin{cases} u_d = -\omega_e L_q i_q, \\ u_q = \omega_e (L_d i_d + \psi_{pm}). \end{cases} \tag{4.18}$$

The function that has to be minimized, the additional task of control algorithm (to provide required torque) and lagrangian can be defined as follows:

$$\begin{aligned} & f(i_d, i_q) = u_d^2 + u_q^2 = \omega_e^2 \left[L_q^2 i_q^2 + (L_d i_d + \psi_{pm})^2 \right] \to \min, \\ & g(i_d, i_q) = T - k_m \left[\psi_{pm} i_q + (L_d - L_q) i_d i_q \right] = 0, \\ & L = \omega_e^2 \left[L_q^2 i_q^2 + (L_d i_d + \psi_{pm})^2 \right] + \lambda \left[T - k_m \psi_{pm} i_q - k_m (L_d - L_q) i_d i_q \right]. \end{aligned} \tag{4.19}$$

According to (4.19), Euler-Lagrange equation can be written as:

$$\begin{cases} \dfrac{\partial L}{\partial i_d} = 2\omega_e^2 L_d (L_d i_d + \psi_{pm}) - \lambda k_m (L_d - L_q) i_q = 0, \\ \dfrac{\partial L}{\partial i_q} = 2\omega_e^2 L_q^2 i_q - \lambda k_T (L_d - L_q) i_q - \lambda k_T \psi_{pm} = 0, \\ \dfrac{\partial L}{\partial i_q} = T - k_T \psi_{pm} i_q - k_T (L_d - L_q) i_d = 0. \end{cases} \tag{4.20}$$

From the first and second equations of (4.20) letting us equate the Lagrange coefficients, as follows:

$$\lambda = \frac{2\omega_e^2 L_d (L_d i_d + \psi_{pm})}{k_T (L_d - L_q) i_q} = \frac{2\omega_e^2 L_q^2 i_q}{k_T \left[(L_d - L_q) i_q + \psi_{pm} \right]}. \tag{4.21}$$

From (4.21) i_d is given by:

$$i_d^2 + \frac{\psi_{pm}}{L_d - L_q} \cdot \frac{2L_d - L_q}{L_d} i_d + \left[\frac{\psi_{pm}^2}{L_d (L_d - L_q)} - \left(\frac{L_q}{L_d} i_q \right)^2 \right], \tag{4.22}$$

after calculation (4.22) we obtain the following equation:

$$i_d = -\frac{\psi_{pm}}{2(L_d - L_q)} \cdot \left(2 - \frac{L_q}{L_d} \right) - \frac{L_q}{L_d} \sqrt{\frac{\psi_{pm}^2}{4(L_d - L_q)^2} - i_q^2}. \tag{4.23}$$

Chapter conclusions

In this chapter, permanent magnet synchronous motor losses were considered and equations for copper and iron losses were defined. Transfer functions of current and speed regulators were determined.

According to PMSM mathematical model, maximum torque per Ampere and maximum torque per Volt control strategies were developed.

The MTPA control algorithm results in the copper losses reduction and is used for speeds below rated.

The MTPV control algorithm results in the iron losses reduction and is used for speeds higher than rated.

CHAPTER 5. MATHEMATICAL SIMULATION OF DEVELOPED ELECTROMECHANICAL SYSTEM

In this chapter developed optimal control algorithms are compared with conventional $i_d = 0$ vector control. Firstly, electromechanical system performance is analyzed for $i_d = 0$, MTPA and MTPV control algorithms. Then the copper and iron losses for all three algorithms are compared.

Though the drivetrain is designed mainly for city usage, its performance has to be tested at a full range of speeds. Therefore, the speed reference trajectory is formed as follows:

1. Vehicle accelerates to set speed $v = 50\ km/h$ with the calculated acceleration $a = 2.78\ m/s^2$ and after that is moving for $5\ s$.
2. Vehicle decelerates with acceleration $a = 2.78\ m/s^2$ to speed $v = 40\ km/h$ and is moving for $5\ s$.
3. Vehicle slows down to complete stop.
4. After $5\ s$ it accelerates to maximum speed $v = 100\ km/h$ and is moving for $5\ s$, then again slows down to a complete stop.

Results of mathematical simulation for $i_d = 0$ the control algorithm are shown in Fig. 5.1.

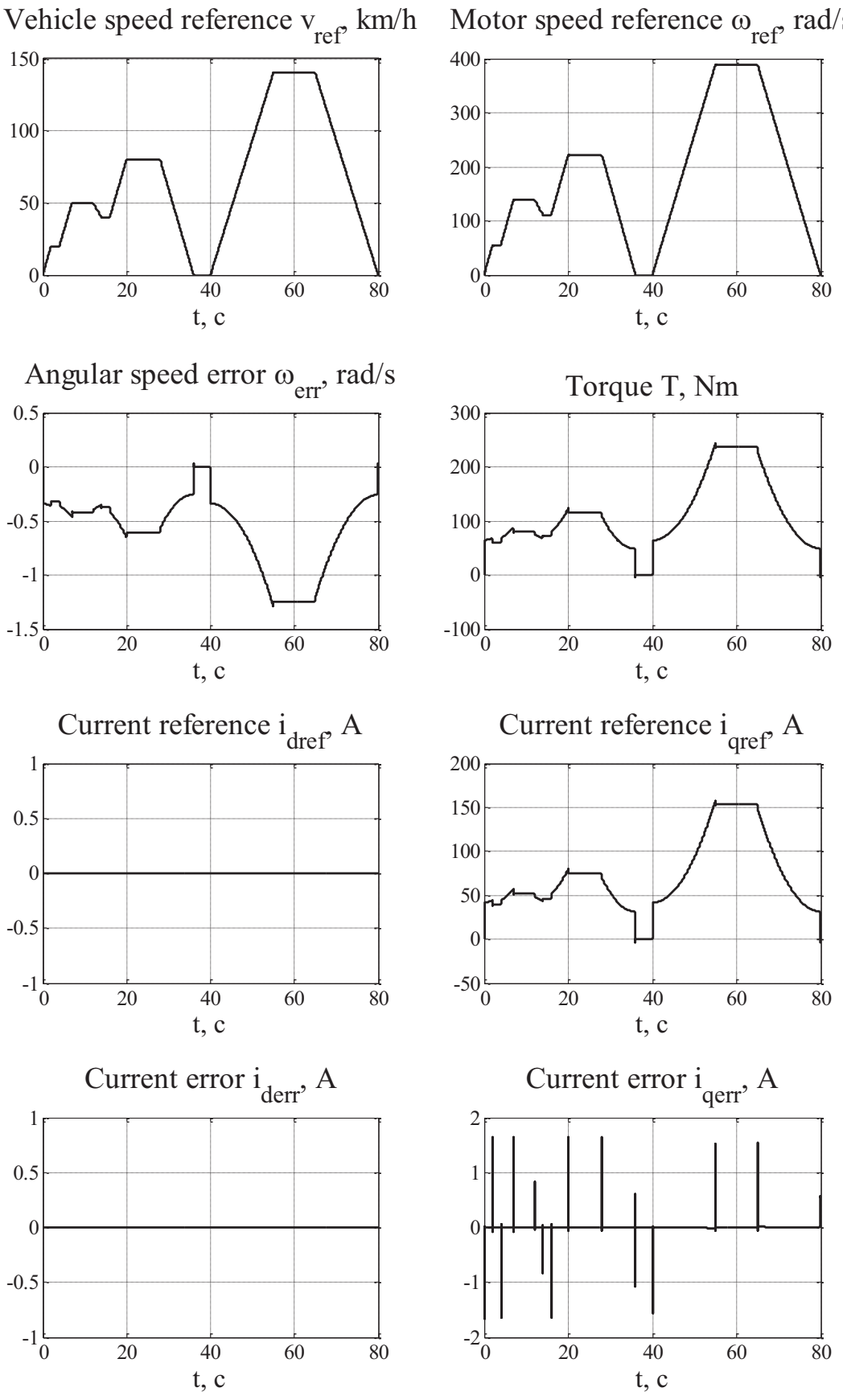

Figure 5.1, a – Modelling results for the $i_d = 0$ control algorithm

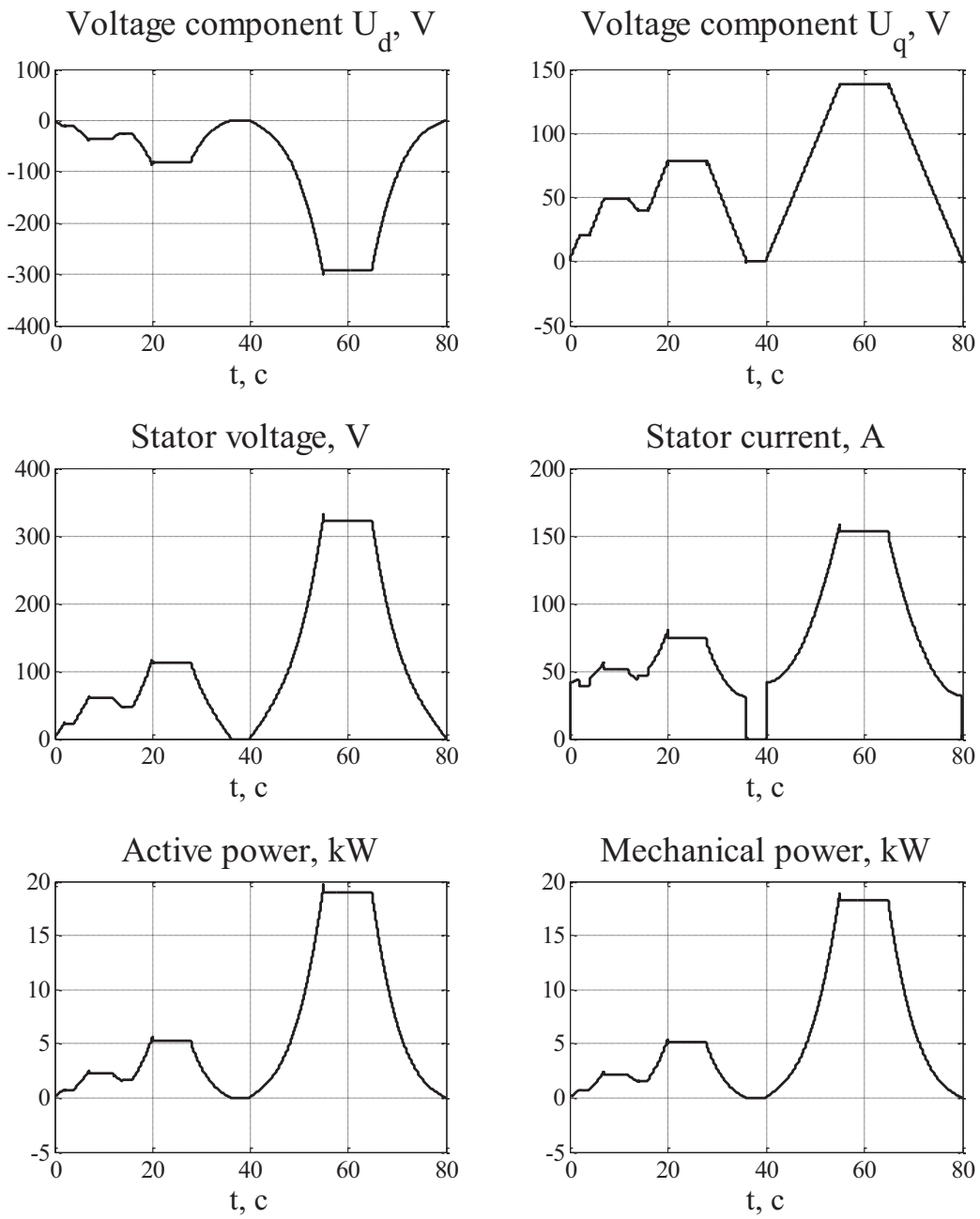

Figure 5.1, b – Modelling results for the $i_d = 0$ control algorithm

From the angular speed error graph in Fig. 5.1, a, it can be seen that the speed reference trajectory is worked out perfectly, only small errors $\omega_{err} = \pm 0.05\ rad/s$ occur during accelerations and decelerations. Motor torque doesn't exceed the rated value.

Since $i_{dref} = 0,$ torque is fully produced by q-axis stator current component which form is identical to torque graph. The current trajectory is worked out perfectly, only small deviations can be seen during transients.

Stator voltage and current do not exceed maximum values, active and mechanical power increases during accelerations due to increased speed and current.

According to the obtained results, developed control algorithm provides required dynamic performance of the traction motor.

Results of mathematical simulation for the MTPA control algorithm are shown in Fig. 5.2.

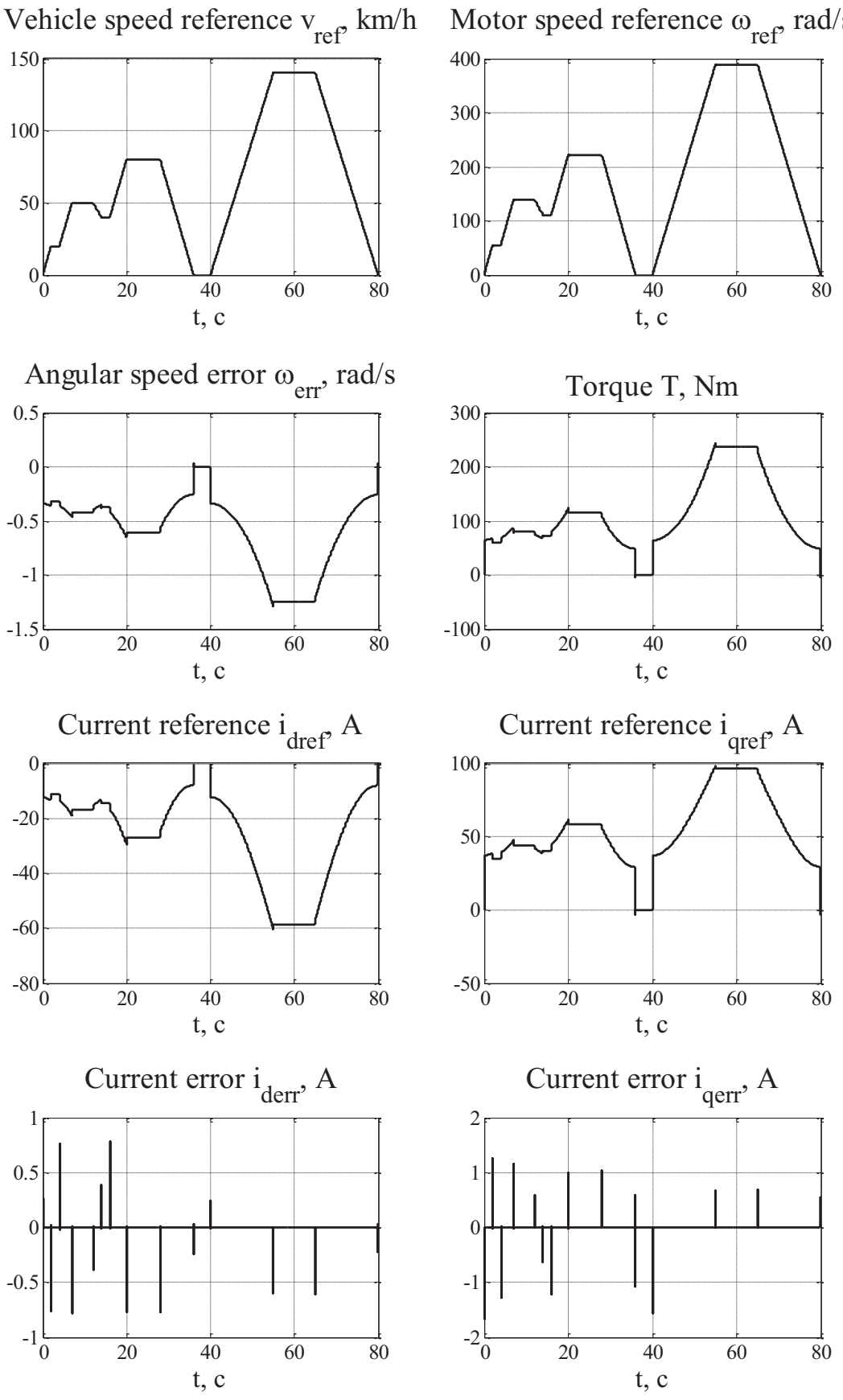

Figure 5.2, a – Modelling results for the MTPA control algorithm

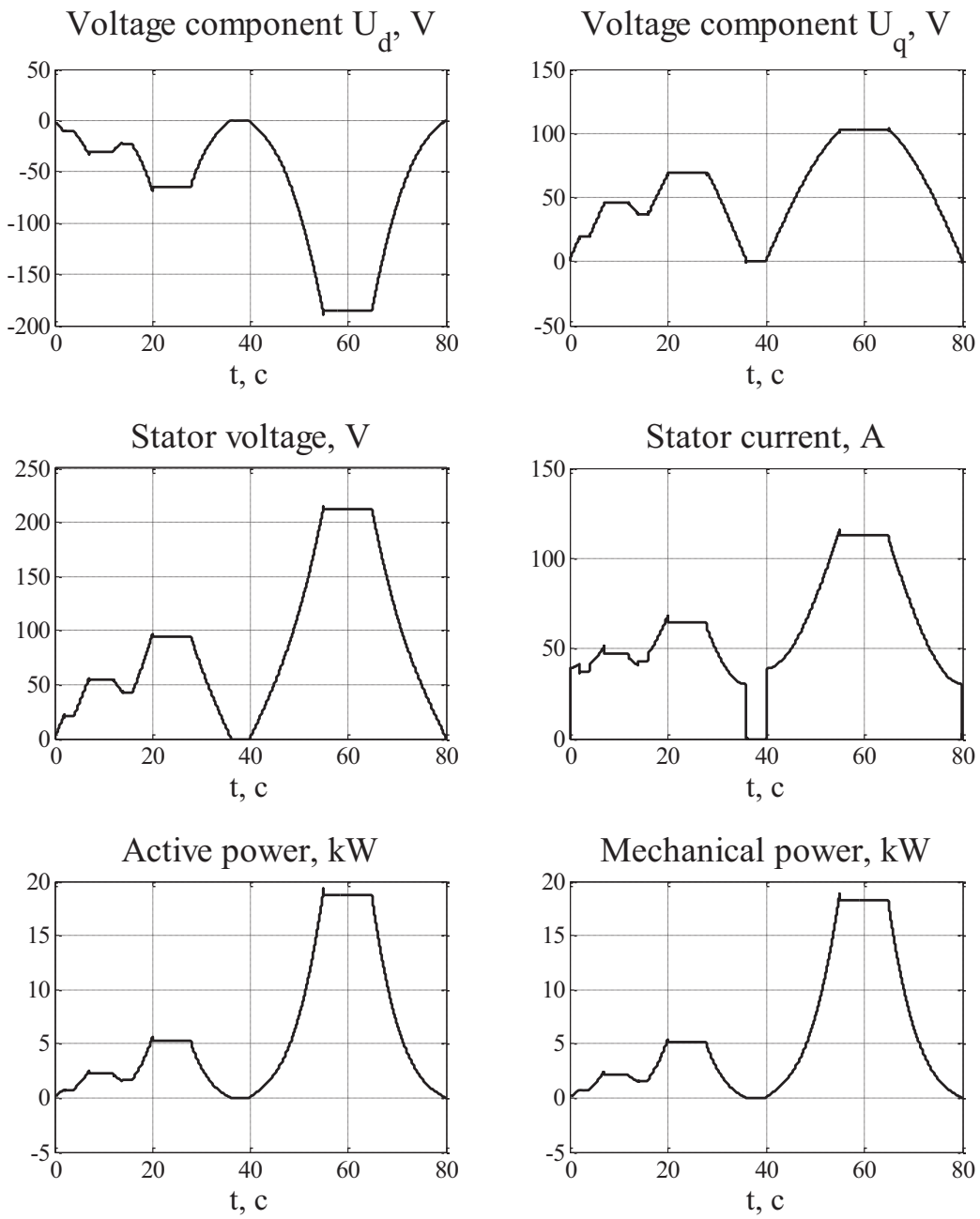

Figure 5.2, b – Modelling results for the MTPA control algorithm

As can be seen from Fig. 5.2, b, speed errors $\omega_{err} = \pm 0.05\ rad/s$ occur during accelerations and decelerations, motor torque doesn't exceed the rated value.

In contrast to the previous method $i_{dref} \neq 0,$ both direct and quadrature stator current components errors occur only in transients and are quickly regulated to zero.

Stator voltage and current don't exceed maximum values, active and mechanical power again increases during accelerations.

According to the obtained results, developed control algorithm provides required dynamic performance of the traction motor.

Results of mathematical simulation for the MTPV control algorithm are shown in Fig. 5.3.

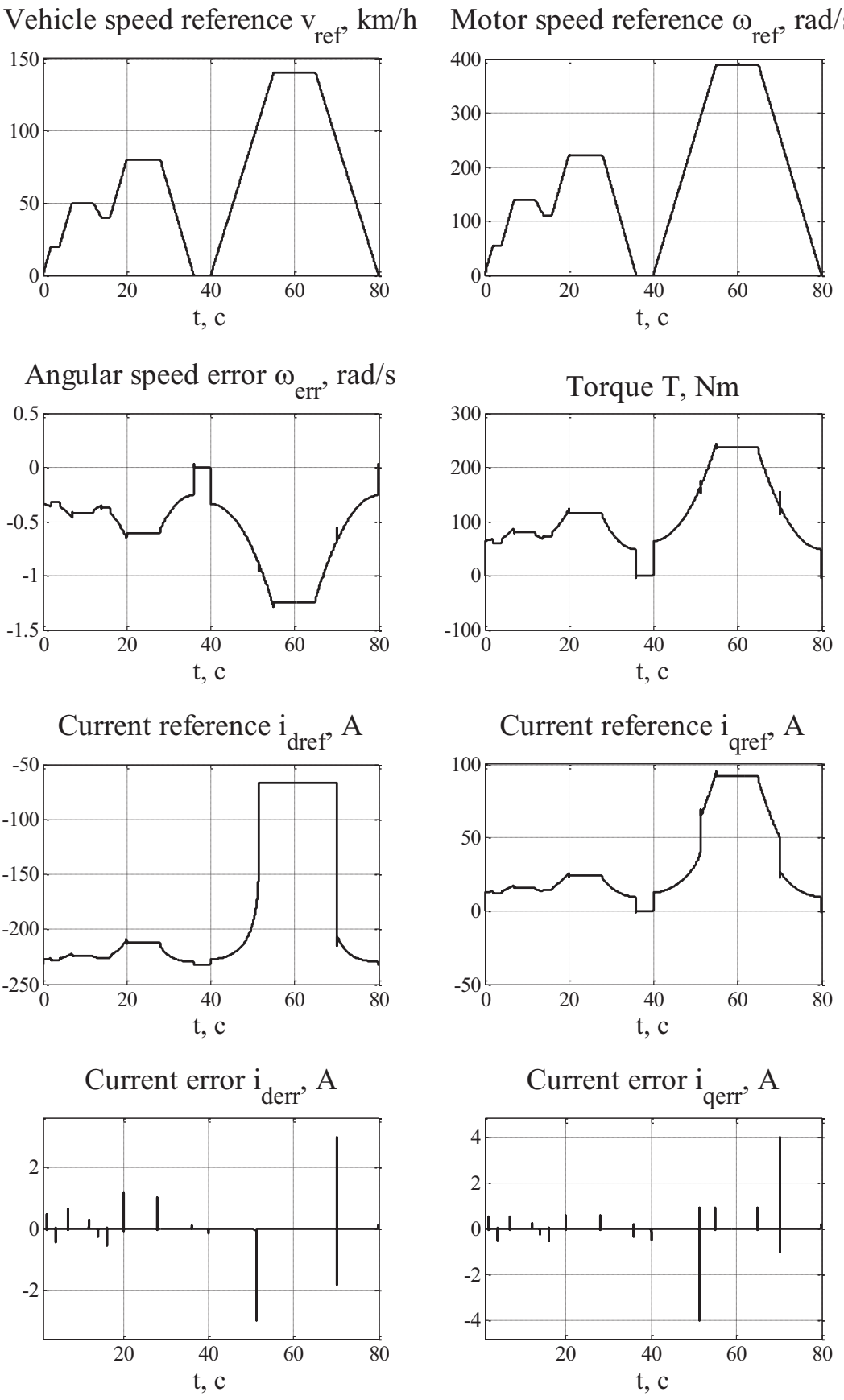

Figure 5.3, a – Modelling results for MTPV control algorithm

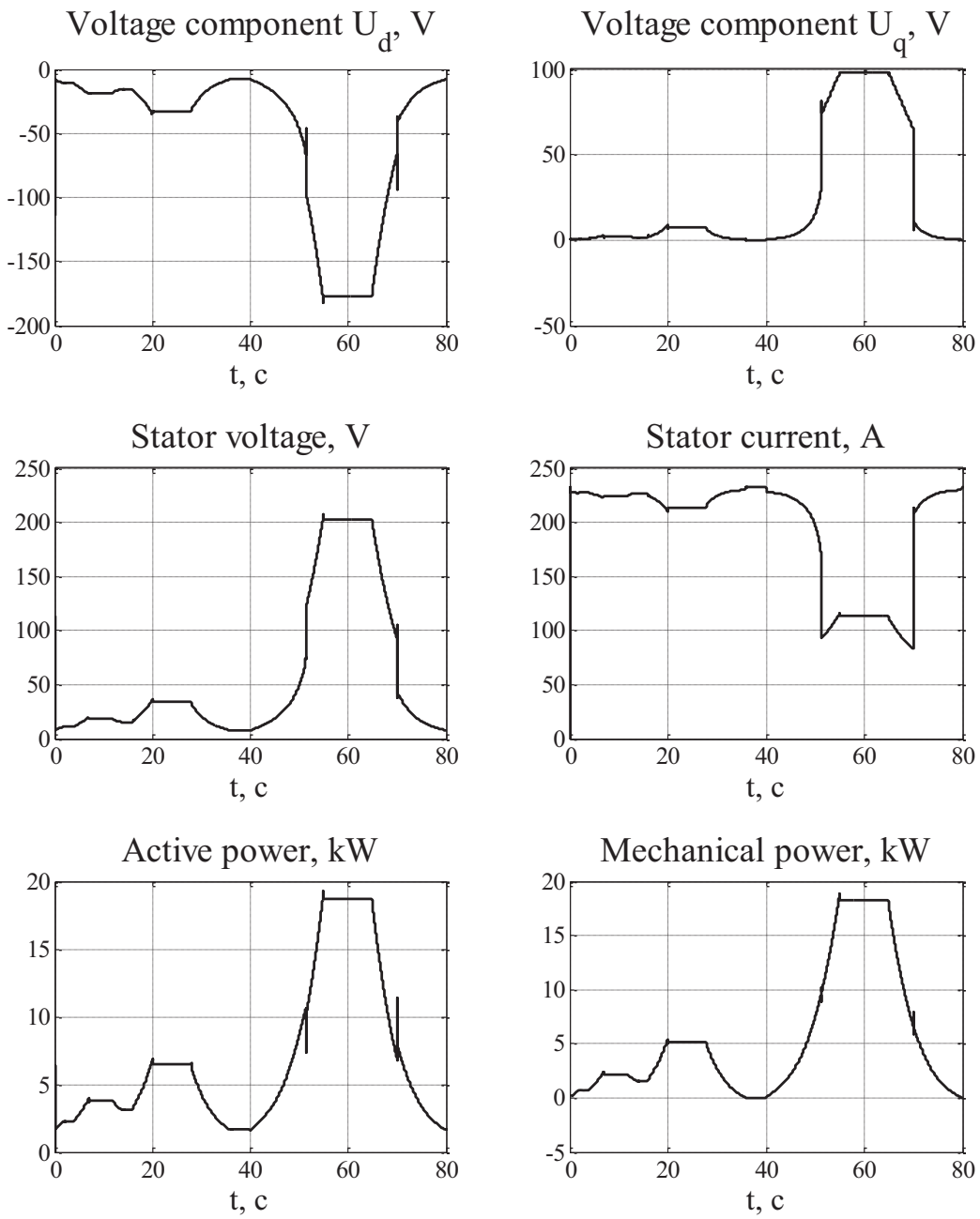

Figure 5.3, b – Modelling results for MTPV control algorithm

From the angular speed error graph in Fig. 5.1, it can be seen that the speed reference trajectory is worked out perfectly, only small errors $\omega_{err} = \pm 1.5\ rad/s$ occur during accelerations to the maximum speed. Motor torque doesn't exceed the rated value.

Both direct and quadrature stator current component errors occur only in transients and are quickly regulated to zero.

Stator voltage and current don't exceed maximum values, active and mechanical power increases during accelerations.

According to the obtained results, developed control algorithm provides required dynamic performance of the traction motor.

To fully analyze control algorithms performance, copper losses according to (4.1) and iron losses according to (4.2) are compared in Fig. 5.4 – 5.5, respectively.

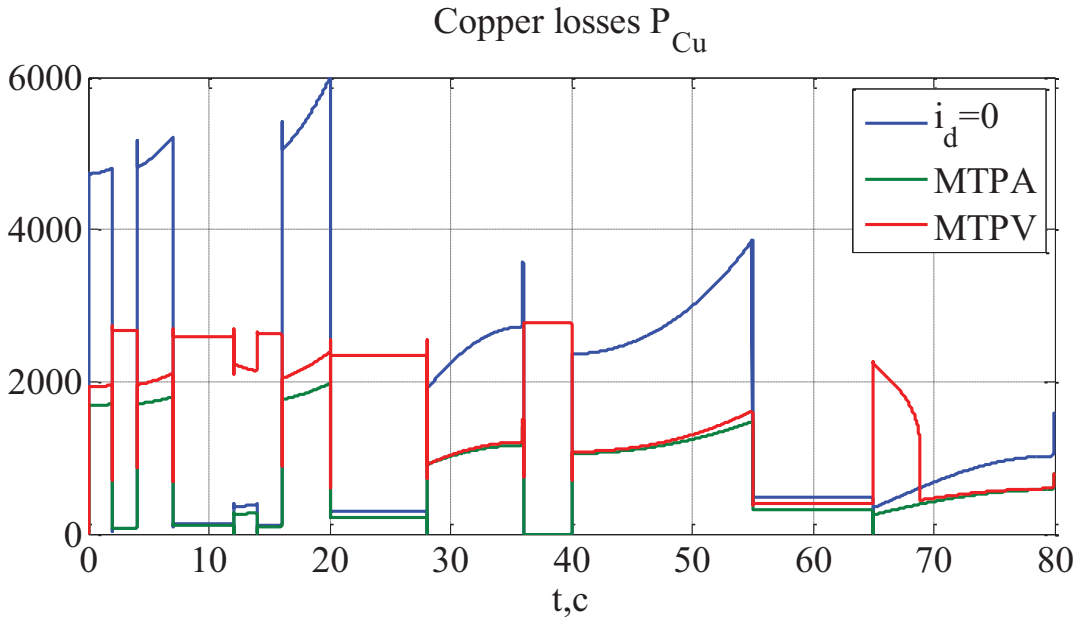

Figure 5.4 – Comparison of copper losses

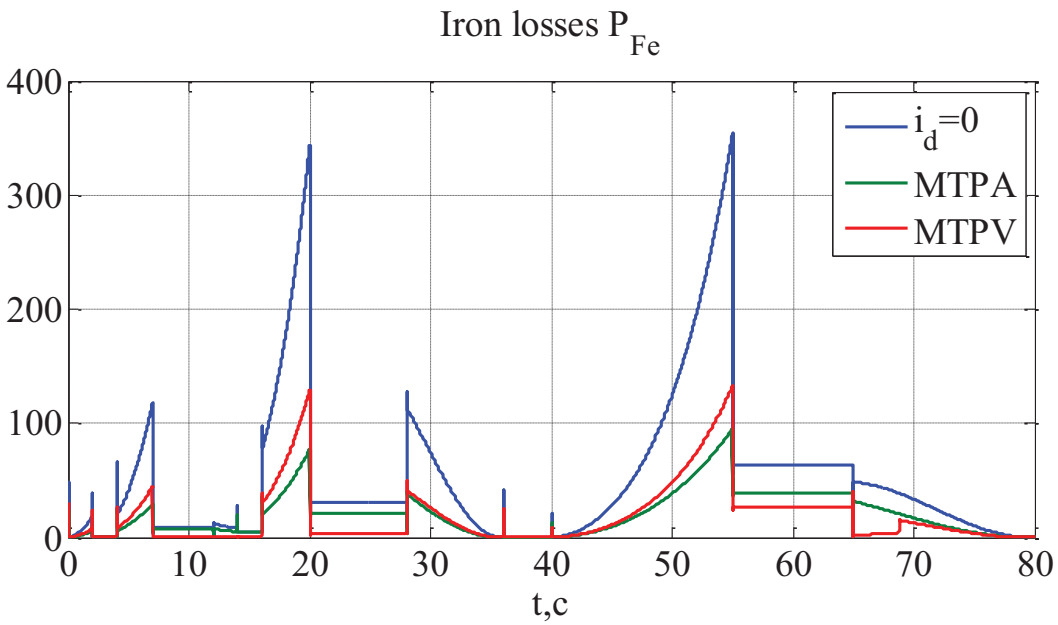

Figure 5.5 – Comparison of iron losses

As can be seen from Fig. 5.4 – 5.5, both MTPA and MTPV strategies allow to significantly reduce copper and iron losses, compared to $i_d = 0$ the method.

MTPA results in copper loss minimization, while MTPV allows for the reduction of iron losses.

Chapter conclusions

In this chapter, developed electromechanical system performance is analyzed via mathematical simulation.

Both optimal control strategies result in significant loss reduction, compared to the conventional $i_d = 0$ vector control method. MTPA strategy provides the highest torque to current ratio, which leads to copper loss minimization.

MTPV algorithm allows to obtain the highest torque to voltage ratio and thereby reduce copper losses. However, current consumption increases, which, in turn, leads to increased copper losses. Moreover, the torque to current ratio is relatively small, hence provided torque is lower at speeds higher than rated.

CHAPTER 6. START-UP DEVELOPMENT

Designed electric drivetrain with a loss minimization control algorithm, based on permanent magnet synchronous motor, can be used in a wide range of electric vehicles. Implementation of this control method allows increasing energy efficiency of the automobile, which makes it possible to expand vehicle power reserve or use the smaller battery pack.

As the global economy is rapidly changing, a firm needs to understand the competitive work environment and identify the appropriate market strategy.

In this chapter, the marketing and economic aspects of startup analysis are presented. Description of the main idea product market entry, its disadvantages, and advantages are presented in Table 6.1-6.2.

Table 6.1 – Short startup description

Idea	Target market	Benefits for customers
Electric vehicle drivetrain, based on IPMSM with loss minimization algorithm	1. Electric vehicles	Greater power reserve, reduced vehicle weight, and lower cost
	2. Public transport	

The next step is to compare our product with already existing products on the market. It was found that potential competitors are electric drivetrains from Infineon [61], Bosch [62], Danfoss [63], and ABB [64]. Infineon and Bosch offer flexible systems for personal electric vehicles, Danfoss provides solutions for both passenger vans and trucks, ABB is mostly focused on working machines and the public transport sector. Thus, Infineon, Bosch, and Danfoss are chosen as three main competitive products, respectively.

Results of strengths and weaknesses analysis are shown in Table 6.2.

Table 6.2 – Product strengths and weaknesses analysis

№	*Technical characteristic*	*Prospective competitive products*				*Weakness*	*Neutral*	*Strength*
		Our product	*Competitor1*	*Competitor2*	*Competitor3*			
1.	Optimal mass-dimensional characteristics	Yes	No	No	No			+
2.	Increased dynamic performance	Yes	No	No	Yes		+	
3.	Ease of maintaining	Yes	No	No	No			+
4.	Cost	Medium	High	High	High		+	

Strengths and weaknesses analysis of the product allows us to estimate its competitiveness in the market. However, since the potential analogs and substitutes parameters are often protected by commercial secrecy, it is quite difficult to make a full comparative analysis.

To estimate the feasibility of product implementation, a technological audit of the project is presented in Table 6.3.

Table 6.3 – Technological audit of the project

№	*Product idea*	*Ways of realization*	*Existence of required technologies*	*Availability of required technologies*
1.	Loss minimization control algorithm implementation	Build-in control algorithms	Existing	Available
		Self-made control algorithms	Existing	Available
2.	Electric drive production and setup	Instruction for self-setup	Should be finished	Available
		Setup by experts	Existing	Available
Selected way of realization: self-made control algorithms usage and set up by the company's experts, since these technologies are available and can be done by the project developer.				

As can be seen, all required technologies are existing and available, so project realization is possible. Market opportunities for the proposed product are listed in Table 6.4-6.15.

Table 6.4 – Preliminary analysis of the market

№	*Market indicators*	*Characteristics*
1	Number of main market players, pcs	3
2	Total sales, UAH/pcs	210000
3	Market dynamics	Growing
4	Market entry restrictions	None
5	Special requirements for certification and standardization	Yes
6	The average market rate of return	ARR=14%

Table 6.5 – Prospective customers analysis

№	*Unmet needs*	*Target customers*	*The difference in perspective target customers behavior*	*Customer requirements*
1.	Mass-dimensional characteristics and dynamic performance of the vehicle have to be improved.	People or firms that use vehicles every day and are interested in fuel economy, environmental protection, money-saving; public transport organizations.	There are no restrictions for customers. However, basic knowledge of EV exploitation would be beneficial.	The electric vehicle should work properly according to the terms of service. Setup by company experts should be ensured.

It is important to highlight that EV appears to be more expensive than conventional internal combustion cars, but it shouldn't be a problem since the availability of the government subsidizing and lending programs. Furthermore, overall technological advancement leads to the price reduction of electric vehicles.

After prospective customer analysis, threats, and opportunities for product market entry should be considered. Results are shown in Table 6.6-6.6, respectively.

Table 6.6 – Threats

№	*Threat*	*Meaning*	*Possible company respond*
1.	Competitiveness	Presence of big companies in the market.	The advertising campaign, offer for a bigger company to buy our product idea.
2.	Price	The high price of the final product.	The search for the cheaper elements for the electric drive to reduce the price of the whole system.

Table 6.6 – Opportunities

№	*Opportunity*	*Meaning*	*Possible company respond*
1.	Growing needs of prospective customers	Modernization of developed propulsion system.	Lineup expanding and/or free maintenance programs.
2.	Improvement of the product quality and elimination of shortcomings, discovered by clients.	Creation of company development strategy.	Cooperation with existing companies, bringing in third-party experts.

The next step is the competitive analysis of the product, given in Table 6.8.

Table 6.8 – Competitive analysis

Competitive environment aspects	*Meaning*	*Possible actions of the company to be competitive*
1. Type of competition - pure	There are at least 4 big companies in the market and a lot of small.	There could be market entry problems. Better relationship with other companies in the market and a good advertisement company are required.
2. Level of competition - international	Our company is from Ukraine, others are European.	Creating a team of specialists for product setting up and testing.
3. Industry ccharacteristic - intra-industry	Products of competitors can be used only in the transport sector.	Focus on quality improvement of the product.
4. Type of product competition - commodity-generic	Competitive products are different, as a different type of propulsion systems are utilized.	Created drivetrain allows for improving mass-dimensional characteristics and dynamic performance.
5. Type of competitive advantage – non-price	EV control algorithms improvement.	Usage of cheaper drivetrain elements to reduce production cost.
6. Type of competitive intensity - branded	Competitors are famous brands in this market sector.	Development of own vehicle lineup or cooperation with other companies.

After competitive analysis, Porter's Five Forces model is used to determine industry structure. This model is widely used to identify the competition intensity of the market [65].

Table 6.9 – Porter's Five Forces

Porter's Five Forces	*Direct rivals in the market*	*Potential of new entrants*	*Suppliers*	*Customers*	*Substitute products*
	List all the direct competitors	*Identify barriers to entry*	*Identify the power of suppliers*	*Identify the power of customers*	*Identify the threat of substitutes*
Conclusions:	There are 3 main competitors in the market. Each rival offers undifferentiated, but not an identical product.	Big brands can be a significant barrier to new entrants.	There are no suppliers, the company directly agrees with the buyer on the terms of purchase and delivery.	Customers can dictate terms and drive the prices down. There is a wide and powerful client base.	There are a few close substitutes on the market, however, their product can be used in place of our company's product.

Taking into account competitive analysis, project idea, and customer needs, justification of competitiveness, and comparative analysis of weaknesses and strengths are presented in Table 6.10-6.11, respectively.

Table 6.10 – Justification of competitiveness

№	*Competitiveness factor*	*Justification*
1.	Better mass-dimensional characteristics	This factor makes the product interesting for the customers since vehicle weight is lower.
2.	Great dynamic performance	This factor makes the product interesting for the customers, since our drivetrain has simpler construction and better performance, in contrast to other rivals.

Table 6.11 – Comparative analysis of weaknesses and strengths

№	*Competitiveness factor*	*Score 1-20*	*Competitive products rating in comparison with our product*						
			–3	*–2*	*–1*	*0*	*+1*	*+2*	*+3*
1.	Better mass-dimensional characteristics	13		+					
2.	Great dynamic performance	16	+						

The last step of product market entry is the SWOT analysis, which makes it possible to evaluate the strategic position of the company. It is done by SWOT matrix creation, which consists of 4 elements: Strengths, Weaknesses, Opportunities, and Threats. Results are given in Table 6.12.

Table 6.12 – SWOT- analysis

Strengths: better mass-dimensional characteristics and dynamic performance.	Weaknesses: relatively high price, existing big brands can be the market entry barriers.
Opportunities: control algorithms improvement, growth of demand.	Threats: competitiveness with big brands, possible price growth because of volatile drivetrain elements cost.

Based on SWOT analysis, market entryways, and implementation time frames are shown in Table 6.13.

Table 6.13 – Ways of market entry

№	*Way*	*Likelihood of resource obtaining*	*Implementation time frames*
1.	Self-made control algorithms usage and set up by the company's experts. This way is faster.	95%	6 months
2.	Built-in control algorithms usage and set up by the company's experts. This way is cheaper, however, dynamic performance can't be improved.	60%	1 year

Following the presented above information, the first way of market entry is chosen, because implementation time frames are shorter and the likelihood of resource obtaining is higher.

The next step in startup development is to choose a market strategy. Thus, target group selection is shown in Table 6.14.

Table 6.14 – Target group selection

№	*Target group*	*Whether a client is ready to buy the product*	*Estimated demand for the target group*	*Competitiveness in the sector*	*Ease of entry*
1.	For personal usage	Price may be high for the buyers, but it can be compensated during operation by higher energy efficiency.	Customers are interested in our EV drivetrain to reduce energy losses.	There are 3 main competitors in the market, however, our product has better characteristics.	Big companies and relatively high cost can be a barrier to market entry.
2.	For commercial usage	Energy efficiency improvement and reduced mass-dimensional characteristics may be interesting for companies.			

It is decided to focus on the production of the system for personal usage since the ability to save money while using the vehicle is more important. The additional target group is organizations, but they may be interested in cooperation with bigger firms.

Development strategy has to be selected to work in chosen sectors. It is shown in Table 6.15.

Table 6.15 – Development strategy selection

№	*Chosen way of development*	*Market coverage strategy*	*Key competitive features of the product*	*Development strategy*
1.	Self-made control algorithms usage and set up by the company's experts, which is a faster way.	Mass marketing.	Better mass-dimensional characteristics and/or better dynamic performance.	Specialization strategy.

Competitive behavior strategy selection is given in Table 6.16.

Table 6.16 – Competitive behavior strategy selection

№	*Is the product a "pioneer" in the market?*	*Will the company attract new customers or take them away from existing competitors?*	*Will the company copy the main parameters of the competitive products?*	*Competitive behavior strategy*
1.	No.	Attract new customers.	Yes, design features to reduce aerodynamic drag.	The strategy of taking a competitive niche in the market.

Then brand positioning strategy has to be selected to identify features, that will attract customers. It is presented in Table 6.16.

Table 6.16 – Brand positioning strategy selection

№	*Target group requirements for product*	*Development strategy*	*Key competitive features of the product*	*Positioning strategy associations of the product*
1.	The electric vehicle should work properly according to the terms of service. Setup by company experts should be ensured.	Specialization strategy.	Better mass-dimensional characteristics and/or better dynamic performance, set up by the company's experts.	Better mass-dimensional characteristics, high dynamic performance.

To develop a startup marketing program, firstly product key benefits should be defined. Results are shown in Table 6.18.

Table 6.18 – Product key benefits

№	*Needs*	*Product benefit*	*Product benefits in comparison with competitors*
1.	Product operating according to the terms of service.	The product was designed to reduce electric losses and ensure a better dynamic performance.	The product is operating by terms of service.
2.	Setup by company experts.	There is a special crew for product setup in the company.	The customer only has to buy the electric vehicle, all set up and testing will be made by company experts.

The three-level marketing model of the product is shown in Table 6.19.

Table 6.19 – Three-level marketing model

Product levels	*Points*
I. Concept of the product	The product is designed for personal everyday usage, setup is made by company experts.
II. Actual product	Features:
	1. High dynamic performance 2. Better mass-dimensional characteristic 3. Ease of maintenance
	Setup and testing will be made by company experts
	No packaging
	Proposed label: EV drivetrain with loss minimization control algorithm
III. Additional service	Before selling: Free test-drive
	After selling: Maintenance done by company experts.
The product will be protected as intellectual property.	

Price range defining is shown in Table 6.20. However, the final price can be set only after a full financial analysis of the project.

Table 6.20 – Price range defining

№	*Substitute products price*	*Direct rivals' price*	*Target group earnings*	*Upper and lower limits of the price range*
1.	240000 UAH	260000 UAH	20000 UAH	220000 UAH

Optimal distribution system selection is given in Table 6.21.

Table 6.21 – Creation of distribution system

№	*Procurement behavior of the target group*	*Function of distributor*	*Sales channels*	*Optimal sale channel*
1.	Customers buy the electric vehicle and pay for non-warranty failures if needed.	Sale	0 – direct, 1 – through one supplier	Direct and resellers.

The final step of startup development is to define the concept of marketing communication, based on previous analysis. The concept is presented in Table 6.22.

Table 6.22 – Concept of marketing communication

№	*Target customers behavior*	*Communication channels, used by customers*	*Product key features*	*Goal of advertisement*	*Concept of the advertising message*
1.	Customers buy electric vehicles for personal everyday usage.	Live communication, Internet	Better mass-dimensional characteristics and/or better dynamic performance, set up by the company's experts.	Show the advantages of the designed product in comparison with direct competitors.	Advertising through the Internet and motor shows.

Chapter conclusions

In this chapter, startup development is presented. Strengths and weaknesses analysis technological audit of the project and competitive analysis are done to select the appropriate product marketing strategy.

The analysis shows that the product should be interesting for personal usage, while there may be difficulties in sales for commercial usage. Since the market is growing, demand also is expected to grow if the right brand positioning strategy and good advertisement campaigns are selected. According to market analysis, it was decided to use self-made control algorithms and set up by the company's experts, because implementation time frames are shorter and the likelihood of resource obtaining is higher.

Existing big brands can be market entry barriers. However, since the proposed project will be protected as intellectual property, offers better mass-dimensional characteristics and dynamic performance, is cheaper than the main competitors, project implementation is expedient.

CONCLUSIONS

In this master thesis, an electric vehicle drivetrain based on a permanent magnet synchronous motor with a loss minimization control algorithm was developed. Obtained electromechanical systems allow increasing the energy efficiency of electric vehicles. The main results of the dissertation are the following:

1. According to the chosen driving cycle and desired vehicle performance, the required equivalent torque of the traction motor and battery pack capacity were determined.
2. Elements of power and control circuits were chosen based on calculated electromechanical system parameters.
3. Loss minimization control algorithm of interior permanent magnet synchronous motor was developed.
4. Both optimal control strategies result in significant loss reduction, compared to the conventional $i_d = 0$ vector control method. MTPA strategy provides the highest torque to current ratio, which leads to copper loss minimization.
5. MTPV algorithm allows to obtain the highest torque to voltage ratio and thereby reduce copper losses. However, current consumption increases, which, in turn, leads to increased copper losses. Moreover, the torque to current ratio is relatively small, hence provided torque is lower at speeds higher than rated.
6. Based on the marketing analysis of the proposed startup, it was determined that project implementation is expedient due to better mass-dimensional characteristics, dynamic performance, and lower price compared to main competitors.

REFERENCES

1. Greenhouse Gas Emissions from a Typical Passenger Vehicle. EPA, 2018 – Retrieved from https://www.epa.gov/greenvehicles/greenhouse-gas-emissions-typical-passenger-vehicle, visited in September 2020.

2. Electric mobility electric motors – mobility & motors pictures of the futureю Siemens, 2013 – Retrieved from www.siemens.com/innovation/en/home/pictures-of-the-future/mobility-and-motors.html, visited in September 2020.

3. 15 % of new cars by 2025 to be at least a hybrid. Green car congress, 2020 – Retrieved from www.greencarcongress.com/hibrid, visited in September 2020.

4. Zeraoulia M., Benbouzid M. Electric Motor Drive Selection Issues for HEV Propulsion Systems: A Comparative Study. IEEE TRANSACTIONS ON INDUSTRIAL ELECTRONICS. 2005. pp. 280–287.

5. Lalit K., Shailendra J. Electric propulsion system for electric vehicular technology: A review. Elsevier. 2014. pp. 924–939.

6. M. Zeraouila, M.E.H. Benbouzid, and D. Diallo. Electric motor drive selection issues for HEV propulsion systems: a comparative study. Vehicle Power and Propulsion, 2005 IEEE Conference.

7. J.F. Gieras, M. Wing, *Permanent Magnet Motor Technology*, ISBN:0-8247-9794-9, Marcel Dekker, New York, 1997

8. Bouaziz, Oussama & Jaafar, Imen & Ammar, Faouzi. (2018). Performance analysis of radial and axial ux PMSM based on 3D FEM modeling. Turkish Journal of Electrical Engineering and Computer Sciences. 26. 10.3906/elk-1708-68.

9. Permanent magnet synchronous motor// Engineering Solutions, 2020 – Retrieved from https://en.engineering-solutions.ru/motorcontrol/pmsm/, visited in September 2020.

10. Z. Biel, J. Vittek, and M. Hrkel. Permanent magnet synchronous motor loss minimization control strategies. 2012 ELEKTRO, Rajeck Teplice, 2012, pp. 165-169.

11. Olga Tolochko (February 13th, 2019). Energy Efficient Speed Control of Interior Permanent Magnet Synchronous Motor, Applied Modern Control, Le Anh Tuan, IntechOpen, DOI: 10.5772/intechopen.80424. Available from: https://www.intechopen.com/books/applied-modern-control/energy-efficient-speed-control-of-interior-permanent-magnet-synchronous-motor

12. L. T. Betí and U. Schäfer. First experimental results of highly efficient permanent magnet synchronous machine for hybrid electric vehicle. Proceedings of the 2011 14th European Conference on Power Electronics and Applications, Birmingham, 2011, pp. 1-8.

13. Chen Y, Fu WN, S HL, Liu H. A quantitative comparison analysis of radial-flux, transverse-flux, and axial-fluxmagnetic gears. IEEE T Magn 2014; 50: 1-4.

14. A. Choudhury, P. Pillay and S. S. Williamson.Modified stator flux estimation based direct torque controlled PMSM drive for hybrid electric vehicle. IECON 2012 - 38th Annual Conference on IEEE Industrial Electronics Society, Montreal, QC, 2012, pp. 2965-2970, doi: 10.1109/IECON.2012.6389425

15. Системи оптимального та інтелектуального керування в електромеханічних системах. Частина 1. Оптимальне керування в електромеханіці. Практикум. [Електронний ресурс]: навч. посіб. для студентів спеціальності 141 «Електроенергетика, електротехніка та електромеханіка» з дисципліни «Системи оптимального та інтелектуального керування»/ О. І. Толочко; КПІ ім. Ігоря Сікорського. – Електронні текстові дані (1 файл: 2198 кБ). Київ: КПІ ім. Ігоря Сікорського, 2019. 116 с.

16. Бешта О.С., Балахонцев О.В., Фурса С.Г. Обгрунтування доцільності використання синхронних двигунів з постійними магнітами з

вбудованими магнітами. Вісник КДУ ім. М. Остроградського. 2010. Вип. 4 ч. 2. – С.73-75.

17. Blaschke F. The principle of field-orientation as applied to the transvector closed loop control system for rotating-field machines: *Siemens Rev*., 34, pp. 217–220, 1972.

18. Li, Jun & Yu, Jia & Chen, Zhenxing. (2013). A Review of Control Strategies for Permanent Magnet Synchronous Motor Used in Electric Vehicles. Applied Mechanics and Materials. 321-324. 1679-1685. 10.4028/www.scientific.net/AMM.321-324.1679.

19. Khaligh A. et al. Battery, ultracapacitor, fuel cell, and hybrid energy storage systems for electric, hybrid electric, fuel cell, and plug-in hybrid electric vehicles: State of the art //IEEE transactions on Vehicular Technology. 2010. Vol. 59. No. 6. pp. 2806-2814.

20. Dhameja S. Electric vehicle battery systems. Elsevier, 2001.

21. Manwell J. F., McGowan J. G. Lead acid battery storage model for hybrid energy systems //Solar Energy. 1993. Т. 50. №. 5. pp. 399-405

22. Ovshinsky S. R., Fetcenko M. A., Ross J. A nickel metal hydride battery for electric vehicles. Science. 1993. Vol. 260. No. 5105. pp. 176-181

23. Notter D. A. et al. Contribution of Li-ion batteries to the environmental impact of electric vehicles. – 2010.

24. Wang J., Sun Z., Wei X. Performance and characteristic research in LiFePO4 battery for electric vehicle applications //Vehicle Power and Propulsion Conference, 2009. VPPC'09. IEEE. – IEEE, 2009. pp. 1657-1661.

25. M.A. Hannan, M.M. Hoque, A. Mohamed, A. Ayob, Review of energy storage systems for electric vehicle applications: Issues and challenges, Renewable and Sustainable Energy Reviews, Volume 69, 2017.

26. Беляков А. И. Электрохимические суперконденсаторы: текущее состояние и проблемы развития. Электрохимическая энергетика. 2006. Т. 6. № 3.

27. ВЫБОР ЭЛЕКТРОДВИГАТЕЛЕЙ ДЛЯ ЭЛЕКТРОМОБИЛЕЙ И ГИБРИДНЫХ АВТОМОБИЛЕЙ В. Д. Мигаль, проф., д.т.н., В. Я. Двадненко, доц., к.т.н., Харьковский национальный автомобильно-дорожный университет, 2016.

28. Chan C.C., Cheng M. (2012) Vehicle Traction Motors. In: Meyers R.A. (eds) Encyclopedia of Sustainability Science and Technology. Springer, New York, NY. https://doi.org/10.1007/978-1-4419-0851-3_800

29. РОЗРОБКА ЕНЕРГОМЕХАНІЧНОЇ УСТАНОВКИ ДЛЯ ТЯГИ ЕЛЕКТРОМОБІЛЯ © Д. Ю. Зубенко, А. В. Коваленко, О. М. Петренко, В. М. Шавкун, М. Ю. Олехно, 2016.

30. Traction Motor Design Considerations, 2020 – Retrieved from http://web.mit.edu/kirtley/www/doe_kirtley_may_2011.pdf, visited in September 2020.

31. Cheng, Ming & Chan, C.C.. (2014). General Requirement of Traction Motor Drives. 10.1002/9781118354179.auto041.

32. Air quality in the world. IQAir, 2020 – Retrieved from https://www.iqair.com/world-air-quality, visited in November 2020.

33. Новый Mini Countryman. Mini, 2020 – Retrieved from https://www.mini.ua/ru_UA/home/range/new-mini-countryman.html #modelselection, visited in October 2020.

34. Mini Countryman 1.5 MT One (02.2017 - 05.2020) - технические характеристики// Дром, 2020 – Retrieved from https://www.drom.ru/catalog/mini/countryman/240148/, visited in October, 2020.

35. Vidal-Bravo, S, De La Cruz-Soto, J, Arrieta Paternina, MR, Borunda, M, Zamora-Mendez, A. Light electric vehicle powertrain: Modeling, simulation, and experimentation for engineering students using PSIM. Comput Appl Eng Educ. 2020; 28: 406– 419. https://doi.org/10.1002/cae.22203

36. Larminie, James & Lowry, John. (2003). Electric Vehicle Technology Explained. 10.1002/0470090707.

37. SKiM459GD12E4// Semikron, 2020 – Retrieved from https://www.semikron.com/products/product-classes/igbt-modules/detail/skim459gd12e4-23930010.html, visited in October 2020.

38. Selecting a IGBT Driver// Design Spark, 2016 – Retrieved from https://www.rs-online.com/designspark/selecting-a-igbt-driver, visited in October 2020.

39. SKYPER 12 press-fit 300A// Semikron, 2020– Retrieved from https://www.semikron.com/products/product-classes/igbt-driver/detail/skyper-12-press-fit-300a-l5066601.html, visited in October 2020.

40. Film Capacitors// TDK, 2018 – Retrieved from https://www.tdk-electronics.tdk.com/inf/20/20/db/fc_2009/MKP_B32674_678.pdf, visited in October 2020.

41. AUTOMOTIVE CURRENT TRANSDUCER OPEN LOOP TECHNOLOGY HAH3DR 700-S03/SP4// LEM, 2019 – Retrieved from https://www.lem.com/sites/default/files/products_datasheets/hah3dr_700_s03_sp4.pdf, visited in October 2020.

42. Current transducers// LEM, 2020 – Retrieved from https://www.lem.com/en/product-list?measurement=52&nominal_val=375-750, visited in October 2020.

43. Buy electronic parts// acdcshop, 2020 – Retrieved from https://www.acdcshop.gr/, visited in October 2020.

44. EMI 55// ELTRA, 2018 – Retrieved from http://www.eltra.it/ products-eltra-encoder-for-motion-control/rotary-incremental-encoders/magnetic-incremental/emi-55-en-gb/, visited in October, 2020.

45. LMx93-N, LM2903-N Low-Power, Low-Offset Voltage, Dual Comparators// Texas Instruments, 2018 – Retrieved from https://www.ti.com/lit/ds/symlink/lm393-n.pdf?ts=1606987136079&ref_url=https%253A%252F%252Fwww.google.de%252F, visited in October 2020.

46. 6N137, VO2601, VO2611, VO2630, VO2631, VO4661// Vishay Semiconductors, 2016 – Retrieved from https://www.vishay.com/docs/84732/6n137.pdf, visited in October 2020.

47. TMS320F28067// Texas Instruments, 2020 – Retrieved from http://www.ti.com/product/TMS320F28067?qgpn=tms320f28067, visited in October, 2020.

48. 161-10.0M-20-25MP Datasheet (PDF) - Oscilent Corporation TMS320F28067// Alldatasheet, 2020 – Retrieved from https://pdf1.alldatasheet.com/datasheet-pdf/view/305063/OSCILENT/161-10.0M-20-25MP.html, visited in October, 2020.

49. TPS75333-EP datasheet DigChip, 2020 – Retrieved from https://www.digchip.com/datasheets/parts/datasheet/477/TPS75333.php, visited in October 2020.

50. AT25010 Datasheet (PDF) - ATMEL Corporation // Alldatasheet, 2020 – Retrieved from https://pdf1.alldatasheet.com/datasheet-pdf/view/56071/ATMEL/AT25010.html, visited in October, 2020.

51. DS1305 Serial Alarm Real-Time Clock// Maxim Integrated, 2015 – Retrieved from https://datasheets.maximintegrated.com/en/ds/DS1305.pdf, visited in October 2020.

52. GENERAL PURPOSE J-FET QUAD OPERATIONAL AMPLIFIERS// ST, 2001 – Retrieved from https://www.egr.msu.edu/eceshop/Parts_Inventory/datasheets/tl084cn.pdf, visited in October 2020.

53. MAX5711 Datasheet (PDF) - Maxim Integrated Products// Alldatasheet, 2020 – Retrieved from https://pdf1.alldatasheet.com/datasheet-pdf/view/73559/MAXIM/MAX5711.html, visited in October 2020.

54. PC814 Series// Sharp, 2020 – Retrieved from http://www.w-r-e.de/robotik/data/opt/pc814.pdf, visited in October 2020.

55. CD74ACT540 Datasheet (PDF) - Texas Instruments // Alldatasheet, 2020 – Retrieved from https://pdf1.alldatasheet.com/datasheet-pdf/view/26929/TI/CD74ACT540.html, visited in October 2020.

56. PC817X Series// Sharp, 2003 – Retrieved from https://www.farnell.com/datasheets/73758.pdf, visited in October 2020.

57. ISO1050 Isolated CAN Transceiver// Texas Instruments, 2019 – Retrieved from https://www.ti.com/lit/ds/symlink/iso1050.pdf?ts=1607156214606&ref_url=https%253A%252F%252Fwww.google.com%252F, visited in October 2020.

58. Low-Power, Slew-Rate-Limited RS-485/RS-422 Transceivers// Maxim Integrated, 2014 – Retrieved from https://datasheets.maximintegrated.com/en/ds/MAX1487-MAX491.pdf, visited in October 2020.

59. Толочко О.І., Божко В.В. Дослідження електроприводів на основі синхронного двигуна з постійними магнітами при оптимальному керуванні за максимумом моменту на ампер. Взрывозащищенное электрооборудование: сб. научн. тр. УкрНИИВЭ. 2010. Донецк: ООО «АИР». С. 242- 247.

60. Vol. 7, Issue 4, April 2018, Comparative Analysis of Cruise Control in Electric Vehicles with PI and Sliding Mode Control, Gopika Vighneswaran1, Keerti.S.Nair2.

61. Electric drive train// Infineon, 2020 – Retrieved from https://www.infineon.com/cms/en/applications/automotive/electric-drive-train/, visited in November 2020.

62. The electric drive// Bosch, 2020 – Retrieved from https://www.bosch-mobility-solutions.com/en/products-and-services/passenger-cars-and-light-commercial-vehicles/powertrain-systems/electric-drive/, visited in November 2020.

63. EDITRON ON-HIGHWAY. Danfoss, 2020 – Retrieved from https://www.danfoss.com/en/about-danfoss/our-businesses/power-solutions/danfoss-editron/editron-on-highway/, visited in November 2020.

64. ABB Powertrain for e-mobility// ABB, 2020 – Retrieved from https://new.abb.com/motors-generators/abb-powertrain-emobility, visited in November 2020.

65. Porter's 5 Forces// Investopedia, 2020 – Retrieved from https://www.investopedia.com/terms/p/porter.asp, visited in December 2020.